FERMILAB-PUB-15-508-T

Published for SISSA by Springer

Received: *December 14, 2015*
Accepted: *January 16, 2016*
Published: *February 18, 2016*

CP violation in heavy MSSM Higgs scenarios

M. Carena,[a,b,c] **J. Ellis,**[d,e] **J.S. Lee,**[f] **A. Pilaftsis**[e,g] **and C.E.M. Wagner**[b,c,h]

[a] *Fermi National Accelerator Laboratory, P.O. Box 500, Batavia IL 60510, U.S.A.*
[b] *Enrico Fermi Institute, University of Chicago, Chicago, IL 60637, U.S.A.*
[c] *Kavli Institute for Cosmological Physics, University of Chicago, Chicago, IL 60637, U.S.A.*
[d] *Theoretical Particle Physics and Cosmology Group, Department of Physics, King's College London, London WC2R 2LS, United Kingdom*
[e] *Theory Division, CERN, CH-1211 Geneva 23, Switzerland*
[f] *Department of Physics, Chonnam National University, 300 Yongbong-dong, Buk-gu, Gwangju, 500-757, Republic of Korea*
[g] *Consortium for Fundamental Physics, School of Physics and Astronomy, University of Manchester, Manchester M13 9PL, United Kingdom*
[h] *HEP Division, Argonne National Laboratory, 9700 Cass Ave., Argonne, IL 60439, U.S.A.*

E-mail: carena@fnal.gov, John.Ellis@cern.ch, jslee@jnu.ac.kr, apostolos.pilaftsis@manchester.ac.uk, cwagner@hep.anl.gov

doi:10.1007/JHEP02(2016)123

JHEP02(2016)123

Operated by Fermi Research Alliance, LLC under Contract No. DE-AC02-07CH11359 with the United States Department of Energy.

Abstract: We introduce and explore new heavy Higgs scenarios in the Minimal Supersymmetric Standard Model (MSSM) with explicit CP violation, which have important phenomenological implications that may be testable at the LHC. For soft supersymmetry-breaking scales M_S above a few TeV and a charged Higgs boson mass M_{H^+} above a few hundred GeV, new physics effects including those from explicit CP violation decouple from the light Higgs boson sector. However, such effects can significantly alter the phenomenology of the heavy Higgs bosons while still being consistent with constraints from low-energy observables, for instance electric dipole moments. To consider scenarios with a charged Higgs boson much heavier than the Standard Model (SM) particles but much lighter than the supersymmetric particles, we revisit previous calculations of the MSSM Higgs sector. We compute the Higgs boson masses in the presence of CP violating phases, implementing improved matching and renormalization-group (RG) effects, as well as two-loop RG effects from the effective two-Higgs Doublet Model (2HDM) scale $M_{H^\pm}$ to the scale M_S. We illustrate the possibility of non-decoupling CP-violating effects in the heavy Higgs sector using new benchmark scenarios named CPX4LHC.

Keywords: Supersymmetry, CP violation, Hadron-Hadron scattering, Higgs physics

ArXiv ePrint: 1512.00437

JHEP02(2016)123

Contents

1 Introduction

Supersymmetry (SUSY) remains one of the best-motivated extensions of the Standard Model (SM), despite the current lack of evidence for supersymmetric partner particles at the LHC. In particular, the discovery of a light Higgs boson in Run I of the LHC, is in agreement with the predictions from SUSY. Supersymmetric theories provide a viable mechanism for stabilizing the electroweak vacuum [1] and require a restricted range for the mass of the lightest Higgs boson [2–4] that contains the measured value [5]. Moreover, minimal low-energy SUSY models with masses of the additional Higgs bosons and supersymmetric particles larger than the weak scale lead to values of the lightest Higgs couplings that are close to the SM ones [6], as suggested by current LHC experiments [7].

On the other hand, the non-discovery of SUSY in Run I of the LHC has disproved benchmark scenarios proposed previously [8], and motivates the consideration of new benchmarks that can be tested in future runs of the LHC. Specifically, it is plausible to consider the case that the common soft SUSY-breaking scale M_S is $\gtrsim 2\,\text{TeV}$, whereas the mass scale M_H of the heavy MSSM Higgs bosons, as determined by the charged Higgs boson mass M_{H^+}, could be somewhat lower, in the few to several hundred GeV range. In relation to this, we recall that future runs of the LHC at 13/14 TeV are expected to be

JHEP02(2016)123

sensitive to squarks and gluinos weighing $\lesssim 3\,\text{TeV}$, and heavy MSSM Higgs bosons weighing $\lesssim 2\,\text{TeV}$ depending on the value of $\tan\beta$. Accordingly, in this paper we introduce and explore MSSM Higgs boson benchmark scenarios with $100\,\text{GeV} \ll M_H \ll M_S \gtrsim 2\,\text{TeV}$.

Our principal interest in new heavy Higgs boson benchmark scenarios is the possible manifestation of observable CP violation in the Higgs sector of the MSSM. It is well known [9–17] that such a possibility arises in the MSSM Higgs potential beyond the tree-level approximation, predominantly from CP phases in the soft SUSY-breaking trilinear couplings of stops and sbottoms, but also from CP phases in the gaugino masses. However, experimental upper limits on electric dipole moments (EDMs) severely constrain the size of such CP-violating parameters as predicted in the MSSM at one-, two- and higher loops [18]. In particular, in the absence of cancellations between these different contributions [19, 20] as occur along specific directions in the space of CP-odd phases [21, 22], the EDM constraints effectively preclude the observation of CP-violating effects in the couplings of the Higgs boson discovered at the LHC [23]. However, the observation of CP violation effects elsewhere, notably in the heavy MSSM Higgs sector [10, 11, 14] or B-meson decays [24, 25] is not excluded. These CP-violating effects have often been studied in the framework of the CPX scenarios proposed previously [8], but in light of the LHC Run-I limits on supersymmetric particle masses and the observed Higgs boson properties, the CPX benchmarks should be revisited.

With the above motivations in mind, in this paper we present new precision calculations of the MSSM Higgs spectrum in the presence of CP violation, which are suitable for scenarios in which the SUSY scale M_S is (far) beyond the TeV region. To this end, we solve the two-loop RGEs of the two-Higgs-doublet model (2HDM) in the range $M_S > Q > M_H$, as well as the two-loop SM RGEs in the range $M_H > Q > m_t^{\text{pole}}$, implementing full one-loop matching conditions at the relevant thresholds M_S, M_H and m_t^{pole}. All the improvements considered here are being implemented in a new version of the public code `CPsuperH` [26–28], namely `CPsuperH3.0`.[1] The full description with all the detailed information about `CPsuperH3.0` will be presented in a future publication.

Section 2 of this paper reviews the conventions and notations of `CPsuperH` that we use for our analysis, as well as some basic formulae for the Higgs boson self-energies. Section 3 specifies the matching conditions and the RG running effects that we incorporate. In section 4 we present some numerical results for the Higgs spectra. In section 5 we introduce our new CP-violating benchmark scenarios (CPX*4*LHC) for the MSSM heavy Higgs sector, and present the results for the CPX*4*LHC benchmarks. Our conclusions are summarized in section 6. The main text of the paper is accompanied by appendices containing detailed formulae: appendix A.1 contains the relevant SM RGEs, appendix A.2 contains the one-loop 2HDM RGEs, appendix A.3 contains the two-loop 2HDM RGEs, and appendix A.4 summarizes the threshold corrections to quartic couplings at the scale M_S.

2 The CP-violating MSSM Higgs sector

In this section we review the computation of the Higgs boson self-energies and pole masses and record the basic expressions used in `CPsuperH3.0`, that underlie our present analysis.

[1] For another tool to calculate CP-violating effects in the MSSM, see [29, 30].

JHEP02(2016)123

We follow the conventions and notations of `CPsuperH` [26–28], unless stated otherwise explicitly.

2.1 The two-Higgs-doublet model (2HDM)

The tree-level 2HDM Higgs potential can be written as [11]:

$$\begin{aligned}\mathcal{L}_V = {} & \mu_1^2\left(\Phi_1^\dagger\Phi_1\right) + \mu_2^2\left(\Phi_2^\dagger\Phi_2\right) + m_{12}^2\left(\Phi_1^\dagger\Phi_2\right) + m_{12}^{*2}\left(\Phi_2^\dagger\Phi_1\right) + \lambda_1\left(\Phi_1^\dagger\Phi_1\right)^2 + \lambda_2\left(\Phi_2^\dagger\Phi_2\right)^2 \\ & + \lambda_3\left(\Phi_1^\dagger\Phi_1\right)\left(\Phi_2^\dagger\Phi_2\right) + \lambda_4\left(\Phi_1^\dagger\Phi_2\right)\left(\Phi_2^\dagger\Phi_1\right) + \lambda_5\left(\Phi_1^\dagger\Phi_2\right)^2 + \lambda_5^*\left(\Phi_2^\dagger\Phi_1\right)^2 \\ & + \lambda_6\left(\Phi_1^\dagger\Phi_1\right)\left(\Phi_1^\dagger\Phi_2\right) + \lambda_6^*\left(\Phi_1^\dagger\Phi_1\right)\left(\Phi_2^\dagger\Phi_1\right) + \lambda_7\left(\Phi_2^\dagger\Phi_2\right)\left(\Phi_1^\dagger\Phi_2\right) + \lambda_7^*\left(\Phi_2^\dagger\Phi_2\right)\left(\Phi_2^\dagger\Phi_1\right).\end{aligned} \tag{2.1}$$

The relations between these and the conventional MSSM parameters are

$$\begin{aligned}&\mu_1^2 = -m_1^2 - |\mu|^2\,, && \mu_2^2 = -m_2^2 - |\mu|^2\,, && \lambda_1 = \lambda_2 = -\frac{1}{8}\left(g^2 + g'^2\right)\,, \\ &\lambda_3 = -\frac{1}{4}\left(g^2 - g'^2\right)\,, && \lambda_4 = \frac{1}{2}\,g^2\,, && \lambda_5 = \lambda_6 = \lambda_7 = 0\,.\end{aligned} \tag{2.2}$$

The doublet Higgs fields may be decomposed as follows:

$$\Phi_1 = \begin{pmatrix} \phi_1^+ \\ \frac{1}{\sqrt{2}}\left(v_1 + \phi_1 + ia_1\right)\end{pmatrix}\,, \qquad \Phi_2 = e^{i\xi}\begin{pmatrix} \phi_2^+ \\ \frac{1}{\sqrt{2}}\left(v_2 + \phi_2 + ia_2\right)\end{pmatrix}\,, \tag{2.3}$$

where the charged and neutral Goldstone bosons, $G^\pm$ and G^0, are determined through the relations:

$$\begin{pmatrix} G^+ \\ H^+\end{pmatrix} = \begin{pmatrix} c_\beta & s_\beta \\ -s_\beta & c_\beta\end{pmatrix}\begin{pmatrix}\phi_1^+ \\ \phi_2^+\end{pmatrix}\,, \qquad \begin{pmatrix} G^0 \\ a\end{pmatrix} = \begin{pmatrix} c_\beta & s_\beta \\ -s_\beta & c_\beta\end{pmatrix}\begin{pmatrix} a_1 \\ a_2\end{pmatrix}\,, \tag{2.4}$$

with $s_\beta \equiv \sin\beta$, $c_\beta \equiv \cos\beta$ and $\tan\beta = v_2/v_1$.

To make contact with the notations used in [31], we make the following identifications: $H_u = \Phi_2$ and $H_d = \widetilde{\Phi}_1 = i\tau_2\Phi_1^* = (\phi_1^{0*}, -\phi_1^-)^T$. Moreover, the kinematic parameters as defined in [31] are related to ours as follows:

$$\begin{aligned}&m_{11}^2 \to -\mu_1^2\,, && m_{22}^2 \to -\mu_2^2\,, && m_{12}^2 \to +m_{12}^2\,, && \\ &\lambda_1 \to -2\lambda_1\,, && \lambda_2 \to -2\lambda_2\,, && \lambda_3 \to -\lambda_3\,, && \lambda_4 \to -\lambda_4\,, \\ &\lambda_5 \to -2\lambda_5\,, && \lambda_6 \to -\lambda_6\,, && \lambda_7 \to -\lambda_7\,, && \\ &g_2 \to g\,, && g_1 \to g' && \cdots && \end{aligned} \tag{2.5}$$

The one-loop 2HDM RGEs are given in appendix A.2,[2] and the two-loop 2HDM RGEs are given in refs. [32, 33] and appendix A.3.

[2] We note that the RGE running parameter used in ref. [31] is related to ours by $t \to 2t$.

JHEP02(2016)123

2.2 Charged Higgs bosons

In the $\{\phi_1^\pm, \phi_2^\pm\}$ basis, the RG-improved charged Higgs-boson self-energy matrix can be found in eq. (2.6) of ref. [16]:

$$\left(\widehat{\Pi}^\pm\right)_{ij}(s) \;=\; -\left(\overline{\mathcal{M}}^2_\pm\right)_{ij} + (\xi_i^+\xi_j^-)^{-1}\left(\Delta\Pi^\pm\right)^{\tilde{f}}_{ij}(s) + \left(\widetilde{\Pi}^\pm\right)^{f}_{ij}(s)\,. \tag{2.6}$$

The first term, $\overline{\mathcal{M}}^2_\pm$, is the two-loop Born-improved squared-mass matrix,

$$\overline{\mathcal{M}}^2_\pm \;=\; \left(\frac{1}{2}\bar{\lambda}_4 v_1 v_2 + \Re\mathrm{e}\overline{m}^2_{12}\right)\begin{pmatrix}\tan\beta & -1\\ -1 & \cot\beta\end{pmatrix}, \tag{2.7}$$

expressed in terms of relevant parameters such as the real part of the soft bilinear Higgs mixing, $\Re\mathrm{e}\overline{m}^2_{12}$, and the quartic coupling λ_4. The bar on these parameters indicates the sum of the tree-level and of the one- and two-loop leading logarithmic contributions. When solving the 2HDM RGEs, $\bar{\lambda}_4$ is to be estimated at the scale M_H where the heavy Higgs bosons decouple, and $\Re\mathrm{e}\overline{m}^2_{12}$ is fixed when the charged-Higgs-boson pole mass is given as an input, as shown below.

The second term in (2.6) describes the threshold effects of the sfermions (top and bottom squarks) and is the product of two quantities: (i) the anomalous dimension factors ξ_i

$$\xi_i = \exp\left[-\int_{\ln M_H}^{\ln M_S}\gamma_i(t)\,\mathrm{d}t\right], \tag{2.8}$$

defined in terms of the anomalous-dimensions of the external Higgs fields $\gamma_i \equiv \mathrm{d}\ln\Phi_i/\mathrm{d}t$ (in this case the charged Higgs fields), and (ii) the scale-invariant one-loop threshold contribution from the top and bottom squarks

$$\left(\Delta\Pi^\pm\right)^{\tilde{f}} \;=\; \left(\frac{1}{2}\lambda_4^{(1)} v_1 v_2 + \Re\mathrm{e}m^{2(1)}_{12}\right)\begin{pmatrix}\tan\beta & -1\\ -1 & \cot\beta\end{pmatrix} + \left(\widetilde{\Pi}^\pm\right)^{\tilde{f}}. \tag{2.9}$$

In the above, the SUSY-breaking scale M_S is used to decouple the heavy sfermions. Moreover, the superscript "(1)" in $\lambda_4^{(1)}$ and $\Re\mathrm{e}m^{2(1)}_{12}$ indicates that these quantities contain the one-loop leading logarithmic contributions and they can be obtained from eqs. (3.6) and (3.7) of [14] by choosing $Q = M_S$.

We note that the vacuum expectation values (VEVs) $v_{1,2}$ of the Higgs doublets $\Phi_{1,2}$, and hence $\tan\beta$, evolve with the wave-function renormalization factors $\xi_{1,2}$ of the corresponding neutral Higgs bosons:

$$v_i(M_S) \;=\; v_i(M_H)/\xi_i\,, \qquad \tan\beta(M_S) \;=\; \tan\beta(M_H)\frac{\xi_1}{\xi_2}\,, \tag{2.10}$$

where $\tan\beta(M_H)$ is the input value of $\tan\beta$, i.e. at the scale $Q = M_H$. Consequently, the SM VEV v is related to the Higgs VEVs $v_{1,2}$ through:

$$v_1(M_H) \;=\; c_\beta(M_H)\,v(M_H)\,, \qquad v_2(M_H) \;=\; s_\beta(M_H)\,v(M_H)\,. \tag{2.11}$$

JHEP02(2016)123

The SM VEV v is fixed at the RG scale $Q = m_t$, by virtue of the relation: $v(M_H) = v(m_t)/\xi_{\rm SM}$, where

$$\xi_{\rm SM} \;=\; \exp\left[-\int_{\ln m_t}^{\ln M_H} \gamma(t)\,{\rm d}t\right] . \tag{2.12}$$

Here $\gamma(t)$ is the anomalous dimension of the SM Higgs doublet, which is given in (A.12) in the one-loop approximation.

Finally, the last terms on the RHSs of (2.9) and (2.6), namely $\left(\widetilde{\Pi}^{\pm}\right)^{\tilde{f}}$ and $\left(\widetilde{\Pi}^{\pm}\right)^{f}$, can be expressed as follows,

$$\left(\widetilde{\Pi}^{\pm}\right)^{\tilde{f}/f} \;=\; \left(\Pi^{\pm}\right)^{\tilde{f}/f} \;+\; \begin{pmatrix} \frac{\left(T_{\phi_1}\right)^{\tilde{f}/f}}{v_1} & i\frac{\left(T_a\right)^{\tilde{f}/f}}{v} \\ -i\frac{\left(T_a\right)^{\tilde{f}/f}}{v} & \frac{\left(T_{\phi_2}\right)^{\tilde{f}/f}}{v_2} \end{pmatrix} , \tag{2.13}$$

with all quantities in the r.h.s. of (2.13) computed in the $\overline{\rm MS}$ scheme. Explicit one-loop calculations yield

$$\begin{aligned} &\left(\Pi^{\pm}\right)^{\tilde{f}} = \Pi^{\pm\,(a)} + \Pi^{\pm\,(b)} , \qquad \left(T_{\phi_{1,2}}\right)^{\tilde{f}} \;=\; T^{(d)}_{\phi_{1,2}} , \qquad \left(T_{a_{1,2}}\right)^{\tilde{f}} \;=\; T^{(d)}_{a_{1,2}} , \\ &\left(\Pi^{\pm}\right)^{f} = \Pi^{\pm\,(c)} , \qquad\qquad\quad \left(T_{\phi_{1,2}}\right)^{f} \;=\; T^{(e)}_{\phi_{1,2}} , \qquad \left(T_{a_{1,2}}\right)^{f} \;=\; 0 , \end{aligned} \tag{2.14}$$

with $T_a = T_{a_2}/c_\beta = -T_{a_1}/s_\beta$ and where $\Pi^{\pm\,(a)}$, $\Pi^{\pm,(b)}$, $\Pi^{\pm\,(c)}$, $T^{(d)}_{\phi_{1,2}}$, $T^{(d)}_{a_{1,2}}$, and $T^{(e)}_{\phi_{1,2}}$ are given by eqs. (B.12), (B.13), (B.15), and (B.16) in [16]. The sfermionic contributions should be calculated at the scale M_S, whereas the fermionic contributions are evaluated at M_H.

In the $\{G^{\pm}, H^{\pm}\}$ basis, the inverse-propagator matrix of the charged Higgs bosons is given by

$$\widehat{\Delta}^{-1}_{\pm}(s) = s\,\mathbf{1}_{2\times 2} + \begin{pmatrix} c_\beta & s_\beta \\ -s_\beta & c_\beta \end{pmatrix} \widehat{\Pi}^{\pm}(s) \begin{pmatrix} c_\beta & -s_\beta \\ s_\beta & c_\beta \end{pmatrix} , \tag{2.15}$$

where we have defined

$$\left(\widehat{\Pi}^{\pm}\right)_{ij}(s) \;=\; -\left(\overline{\mathcal{M}}^2_{\pm}\right)_{ij} + \left(\Delta\widehat{\Pi}^{\pm}\right)_{ij}(s) . \tag{2.16}$$

In (2.15), the $\{22\}$ matrix element of the second term is given by

$$\begin{aligned} &\left(\widehat{\Pi}^{\pm}\right)_{11} s^2_\beta - \left[\left(\widehat{\Pi}^{\pm}\right)_{12} + \left(\widehat{\Pi}^{\pm}\right)_{21}\right] s_\beta c_\beta + \left(\widehat{\Pi}^{\pm}\right)_{22} c^2_\beta \\ &= -\left(\frac{1}{2}\bar{\lambda}_4 v^2 + \frac{\Re{\rm e}\overline{m}^2_{12}}{c_\beta s_\beta}\right) + \Delta\widehat{\Pi}_{H^+H^-} , \end{aligned} \tag{2.17}$$

with

$$\Delta\widehat{\Pi}_{H^+H^-} \;\equiv\; \left(\Delta\widehat{\Pi}^{\pm}\right)_{11} s^2_\beta - \left[\left(\Delta\widehat{\Pi}^{\pm}\right)_{12} + \left(\Delta\widehat{\Pi}^{\pm}\right)_{21}\right] s_\beta c_\beta + \left(\Delta\widehat{\Pi}^{\pm}\right)_{22} c^2_\beta . \tag{2.18}$$

This yields the pole mass condition

$$\begin{aligned} &\Re{\rm e}\left(\widehat{\Delta}^{-1}_{\pm}\right)_{22}(s = M^2_{H^\pm}) \\ &= M^2_{H^\pm} \;-\; \left(\frac{1}{2}\bar{\lambda}_4 v^2 \;+\; \frac{\Re{\rm e}\overline{m}^2_{12}}{c_\beta s_\beta}\right) \;+\; \Re{\rm e}\Delta\widehat{\Pi}_{H^+H^-}(s = M^2_{H^\pm}) \;=\; 0 , \end{aligned} \tag{2.19}$$

which may be used to eliminate $\Re{\rm e}\overline{m}^2_{12}$ in favor of the charged-Higgs boson pole mass $M^2_{H^\pm}$.

JHEP02(2016)123

2.3 Neutral Higgs bosons

In the $\{\phi_1, \phi_2, a_1, a_2\}$ basis, eq. (2.14) of [16] takes the form

$$\widehat{\Pi}^N(s) \;=\; \begin{pmatrix} \widehat{\Pi}^S(s) & \widehat{\Pi}^{SP}(s) \\ \left(\widehat{\Pi}^{SP}(s)\right)^T & \widehat{\Pi}^P(s) \end{pmatrix}, \tag{2.20}$$

with

$$\begin{aligned}
\left(\widehat{\Pi}^S\right)_{ij}(s) &= -\left(\overline{\mathcal{M}}_S^2\right)_{ij} + (\xi_i\xi_j)^{-1}\left(\Delta\Pi^S\right)^{\tilde{f}}_{ij}(s) + \left(\widetilde{\Pi}^S\right)^{f}_{ij}(s)\,, \\
\left(\widehat{\Pi}^P\right)_{ij}(s) &= -\left(\overline{\mathcal{M}}_P^2\right)_{ij} + (\xi_i\xi_j)^{-1}\left(\Delta\Pi^P\right)^{\tilde{f}}_{ij}(s) + \left(\widetilde{\Pi}^P\right)^{f}_{ij}(s)\,, \\
\left(\widehat{\Pi}^{SP}\right)_{ij}(s) &= (\xi_i\xi_j)^{-1}\left(\widetilde{\Pi}^{SP}\right)^{\tilde{f}}_{ij}(s) + \left(\widetilde{\Pi}^{SP}\right)^{f}_{ij}(s)\,.
\end{aligned} \tag{2.21}$$

where, in analogy with eq. (2.8), ξ_i are the corresponding anomalous dimension factors of the neutral Higgs fields.

The quantities $\overline{\mathcal{M}}_S^2$ and $\overline{\mathcal{M}}_P^2$ appearing here may be written in the forms

$$\begin{aligned}
\overline{\mathcal{M}}_S^2 &= \Re\mathrm{e}\overline{m}_{12}^2 \begin{pmatrix} \tan\beta & -1 \\ -1 & \cot\beta \end{pmatrix} - v^2 \begin{pmatrix} 2\bar{\lambda}_1 c_\beta^2 & \bar{\lambda}_{34} c_\beta s_\beta \\ \bar{\lambda}_{34} c_\beta s_\beta & 2\bar{\lambda}_2 s_\beta^2 \end{pmatrix}, \\
\overline{\mathcal{M}}_P^2 &= \Re\mathrm{e}\overline{m}_{12}^2 \begin{pmatrix} \tan\beta & -1 \\ -1 & \cot\beta \end{pmatrix},
\end{aligned} \tag{2.22}$$

where $\bar{\lambda}_1$, $\bar{\lambda}_2$, and $\bar{\lambda}_{34} = \bar{\lambda}_3 + \bar{\lambda}_4$ are to be evaluated by solving the 2HDM RGEs at the scale M_H.

The quantities $\Delta\Pi^S$ and $\Delta\Pi^P$ may be written as

$$\begin{aligned}
\left(\Delta\Pi^S\right)^{\tilde{f}} &= \Re\mathrm{e}m_{12}^{2(1)} \begin{pmatrix} t_\beta & -1 \\ -1 & 1/t_\beta \end{pmatrix} - v^2 \begin{pmatrix} 2\lambda_1^{(1)} c_\beta^2 & \lambda_{34}^{(1)} c_\beta s_\beta \\ \lambda_{34}^{(1)} c_\beta s_\beta & 2\lambda_2^{(1)} s_\beta^2 \end{pmatrix} + \left(\widetilde{\Pi}^S\right)^{\tilde{f}}, \\
\left(\Delta\Pi^P\right)^{\tilde{f}} &= \Re\mathrm{e}m_{12}^{2(1)} \begin{pmatrix} t_\beta & -1 \\ -1 & 1/t_\beta \end{pmatrix} + \left(\widetilde{\Pi}^P\right)^{\tilde{f}},
\end{aligned} \tag{2.23}$$

where $\lambda_{1,2,34}^{(1)}$ and $\Re\mathrm{e}m_{12}^{2(1)}$ can be obtained from eqs. (3.3), (3.4), (3.5), (3.6) and (3.7) of [14] by choosing $Q = M_S$.

The quantities $\widetilde{\Pi}^{S,P,SP}$ are given in the $\overline{\mathrm{MS}}$ scheme by eq. (2.11) of [16]:

$$\begin{aligned}
\widetilde{\Pi}^S &= \Pi^S + \begin{pmatrix} \frac{T_{\phi_1}}{v_1} & 0 \\ 0 & \frac{T_{\phi_2}}{v_2} \end{pmatrix}, \\
\widetilde{\Pi}^{SP} &= \Pi^{SP} + \frac{T_a}{v} \begin{pmatrix} 0 & +1 \\ -1 & 0 \end{pmatrix}, \\
\widetilde{\Pi}^P &= \Pi^P + \begin{pmatrix} \frac{T_{\phi_1}}{v_1} & 0 \\ 0 & \frac{T_{\phi_2}}{v_2} \end{pmatrix}.
\end{aligned} \tag{2.24}$$

JHEP02(2016)123

Here, $\left(\Pi^S\right)^{\tilde{f}}$ and $\left(\Pi^S\right)^{f}$ are given by

$$\left(\Pi^S\right)^{\tilde{f}} = \Pi^{S,(a)} + \Pi^{S,(b)}\,, \qquad \left(\Pi^S\right)^{f} = \Pi^{S,(c)}\,, \tag{2.25}$$

which are specified in eqs. (B.5), (B.6), and (B.14) of [16]. In addition, $\left(\Pi^P\right)^{\tilde{f}}$ and $\left(\Pi^P\right)^{f}$ are given by

$$\left(\Pi^P\right)^{\tilde{f}} = \Pi^{P,(a)} + \Pi^{P,(b)}\,, \qquad \left(\Pi^P\right)^{f} = \Pi^{P,(c)}\,,$$

which can be obtained from eqs. (B.5), (B.6) by replacing $\phi_i \to a_i$ and from eq. (B.14) of [16]. Moreover, the CP-violating self-energies $\left(\Pi^{SP}\right)^{\tilde{f}}$ and $\left(\Pi^{SP}\right)^{f}$ may be expressed as

$$\left(\Pi^{SP}\right)^{\tilde{f}} = \Pi^{SP,(a)}\,, \qquad \left(\Pi^{SP}\right)^{f} = 0\,. \tag{2.26}$$

The non-zero self-energy $\Pi^{SP,(a)}$ is given by eq. (B.11) of [16].

Finally, the inverse propagator matrix of the neutral Higgs bosons in the $\{\phi_1, \phi_2, a, G^0\}$ basis is given by

$$\widehat{\Delta}_N^{-1}(s) = s\,\mathbf{1}_{4\times 4} + \begin{pmatrix} 1 & 0 & 0 & 0 \\ 0 & 1 & 0 & 0 \\ 0 & 0 & -s_\beta & c_\beta \\ 0 & 0 & c_\beta & s_\beta \end{pmatrix} \widehat{\Pi}^N(s) \begin{pmatrix} 1 & 0 & 0 & 0 \\ 0 & 1 & 0 & 0 \\ 0 & 0 & -s_\beta & c_\beta \\ 0 & 0 & c_\beta & s_\beta \end{pmatrix}\,, \tag{2.27}$$

and the physical masses can be obtained from the pole-mass conditions. We should reiterate here that the parameter $\tan\beta$ is defined at $s = 0$. In this kinematic limit, the Goldstone boson G^0 decouples from the 4×4 propagator matrix, independently of the presence of explicit CP violation in the theory [9], as a consequence of the Goldstone theorem.

3 Matching conditions and RG running effects

Here we detail the $\overline{\rm MS}$ renormalization group approach that we follow for the computation of the masses and mixings of the neutral and charged Higgs bosons in the CP-violation case. In particular, we state explicitly our matching conditions at the relevant threshold scales. Given these matching conditions, we compute the RG running effects to the relevant gauge, Yukawa and quartic couplings between the different threshold scales.

To start with, we define the SUSY-breaking scale M_S by

$$M_S^2 \;\equiv\; \max\left(M_{\tilde{Q}_3}^2 + m_t^2, M_{\tilde{U}_3}^2 + m_t^2,\; M_{\tilde{D}_3}^2 + m_b^2, M_{\tilde{L}_3}^2 + m_\tau^2,\; M_{\tilde{E}_3}^2 + m_\tau^2\right)\,, \tag{3.1}$$

which acts as the SUSY threshold scale. For the purposes of this study, we ignore possible hierarchies between the third-generation sfermions, by assuming they are small as compared to the other two hierarchical scales: (i) the heavy Higgs-sector scale $M_H \equiv M_{H^+}$; (ii) the top-quark mass m_t.

JHEP02(2016)123

The matching conditions for the quartic and Yukawa couplings at the threshold M_S are as follows:

$$\begin{aligned}
\bar{\lambda}_1 = \bar{\lambda}_2 \;&=\; -\frac{1}{8}\left(g^2+g'^2\right), \qquad \bar{\lambda}_3 = -\frac{1}{4}\left(g^2-g'^2\right), \qquad \bar{\lambda}_4 = \frac{1}{2}\,g^2\,; \\
h_t^{\rm MSSM} &= \frac{h_t^{\rm 2HDM}}{1+\delta_t+\cot\beta\Delta_t}\,, \\
h_b^{\rm MSSM} &= \frac{h_b^{\rm 2HDM}}{1+\delta_b+\tan\beta\Delta_b}\,, \\
h_\tau^{\rm MSSM} &= \frac{h_\tau^{\rm 2HDM}}{1+\tan\beta\Delta_\tau}\,,
\end{aligned} \tag{3.2}$$

where $\Delta_f = \Delta h_f/h_f^{\rm MSSM}$, $\delta_f = \delta h_f/h_f^{\rm MSSM}$, and Δh_f and δh_f are the supersymmetric threshold corrections to the third generation Yukawa couplings [14, 34]. The difference between δh_f and Δh_f is that δh_f is a radiative correction to the supersymmetric $h_f^{\rm MSSM}$ coupling of up-quarks, down-quarks and leptons. The coupling Δh_f, instead, is a loop-induced coupling of the fermions to the Higgs doublet to which they do not couple in the supersymmetric limit. Therefore, below the scale M_S the theory becomes a general 2HDM, with up-quarks coupled to Φ_2 and down-quarks and leptons coupled to Φ_1, with couplings given by $h_f^{\rm MSSM}(1+\delta_f)$, respectively, but with additional loop-induced couplings Δh_f to the other Higgs doublet. The couplings $h_f^{\rm 2HDM}$ are the combinations of these Yukawa couplings related to the running fermion masses in the same way as in a Type-II 2HDM. Notice that in the present approach, we treat the loop-induced couplings Δh_f as small departures from a Type-II 2HDM. Hence, we are working in a Type-II approximation to a general 2HDM.

The RGEs for the 2HDM used for $M_S > Q > M_H$ are described in appendices A.2 and A.3. At the heavy Higgs threshold $M_H \equiv M_{H^\pm}$, the following matching conditions are employed:

$$\begin{aligned}
\lambda &= \frac{\left(M_{H_1}^{\rm EP}\right)^2}{v^2} - \frac{1}{16}\kappa\left(g^2+g'^2\right)^2 s_{4\beta}^2\,, \\
h_t^{\rm 2HDM} &= \frac{y_t}{s_\beta}\,, \qquad h_b^{\rm 2HDM} = \frac{y_b}{c_\beta}\,, \qquad h_\tau^{\rm 2HDM} = \frac{y_\tau}{c_\beta}\,,
\end{aligned} \tag{3.3}$$

where $M_{H_1}^{\rm EP}$ denotes the effective potential mass of the lightest neutral Higgs boson calculated in the limit of zero external momentum $s = 0$. In the above, we have ignored the small effects due to scheme conversion from dimensional regularization to dimensional reduction [35]. In practice, while evaluating the evolution of the gauge, Yukawa and quartic couplings, at $M_H < Q < M_S$, we have assumed an effective Type-II 2HDM, in which the Yukawa couplings are given by $h_f^{\rm 2HDM}$ with the matching condition, eq. (3.3) given at the scale M_H. As already mentioned above, this amounts to an approximate treatment of the loop-induced Δh_f effects on the computation of the Higgs boson masses and mixing angles.

At scales below the heavy Higgs scale M_H, the only physical degrees of freedom are the SM ones. The RGEs for the SM used for $Q < M_H$ are described in appendix A.1. We

JHEP02(2016)123

define the SM Higgs potential as

$$V(\Phi) \;=\; -\frac{m^2}{2}|\Phi|^2 \;+\; \frac{\lambda}{2}|\Phi|^4\,,$$

with $\Phi = (0,(v+h)/\sqrt{2})^T$ and $\lambda = m^2/v^2$. Note that the quartic coupling of Φ is defined with a factor (-2) difference compared to the quartic couplings of $\Phi_{1,2}$ in eq. (2.1). In order to compare with the experimental results, it is important to define the SM boundary conditions for the gauge, Yukawa and quartic couplings. In our work we use [36]

$$\begin{aligned}
y_t &= 0.93697 + 0.00550\left(\frac{m_t^{\rm pole}}{\rm GeV} - 173.35\right) - 0.00042\frac{\alpha_s(M_Z)-0.1184}{0.0007}\,,\\
g_s &= 1.1666 + 0.00314\frac{\alpha_s(M_Z)-0.1184}{0.0007} - 0.00046\left(\frac{m_t^{\rm pole}}{\rm GeV} - 173.35\right)\,,\\
g' &= 0.3587\,, \quad g = 0.6483\,, \quad y_b = 0.0156\,, \quad y_\tau = 0.0100\,.
\end{aligned} \tag{3.4}$$

The pole mass-squared of the lightest Higgs boson is then given by [35]:

$$\begin{aligned}
\left(M_{H_1}^{\rm pole}\right)^2 &= \lambda\left(m_t^{\rm pole}\right)\, v^2\left(m_t^{\rm pole}\right)\\
&+\kappa\Big\{3y_t^2\left(4\overline{m}_t^2 - m_h^2\right)B_0\left(m_h^2,\overline{m}_t^2,\overline{m}_t^2\right) - \frac{9}{2}\lambda m_h^2\left[2 - \frac{\pi}{\sqrt{3}} - \log\frac{m_h^2}{Q_{\rm RG}^2}\right]\\
&-\frac{v^2}{4}\left[3g^4 - 4\lambda g^2 + 4\lambda^2\right]B_0\left(m_h^2, M_W^2, M_W^2\right)\\
&-\frac{v^2}{8}\left[3\left(g^2+g'^2\right)^2 - 4\lambda\left(g^2+g'^2\right) + 4\lambda^2\right]B_0\left(m_h^2, M_Z^2, M_Z^2\right)\\
&+\frac{1}{2}g^4\left[g^2 - \lambda\left(\log\frac{M_W^2}{Q_{\rm RG}^2} - 1\right)\right] + \frac{1}{4}\left(g^2+g'^2\right)\left[\left(g^2+g'^2\right) - \lambda\left(\log\frac{M_Z^2}{Q_{\rm RG}^2} - 1\right)\right]\Big\}\,,
\end{aligned} \tag{3.5}$$

where $\overline{m}_t = y_t v/\sqrt{2}$ and $m_h^2 = \lambda(m_t^{\rm pole})\, v^2(m_t^{\rm pole})$. We take the renormalization group scale $Q_{\rm RG} = m_t^{\rm pole}$, and the function B_0 used in (3.5) is defined in [16].

4 Numerical results for the MSSM Higgs sector

We first illustrate the effects of the RG running in the range of scales $Q > M_H$ using a specific scenario with universal SUSY parameters fixed to be 1 TeV:

$$\mu \;=\; M_{1,2,3} \;=\; M_{\tilde{Q}_3,\tilde{U}_3,\tilde{D}_3,\tilde{L}_3,\tilde{E}_3} \;=\; A_{t,b,\tau} \;=\; 1\ {\rm TeV}\,, \qquad \rho_{\tilde{Q},\tilde{U},\tilde{D},\tilde{L},\tilde{E}} \;=\; 1\,, \tag{4.1}$$

where $\rho_{\tilde{Q}} = M_{\tilde{Q}_{1,2}}/M_{\tilde{Q}_3}$, $\rho_{\tilde{U}} = M_{\tilde{U}_{1,2}}/M_{\tilde{U}_3}$, etc, and we have assumed no hierarchy between the three generations of sfermion masses.

Figure 1 illustrates with black lines the one-loop running of the 2HDM quartic couplings up to $Q = 10^6$ GeV in the above scenario, eq. (4.1), and compares them with the running of

JHEP02(2016)123

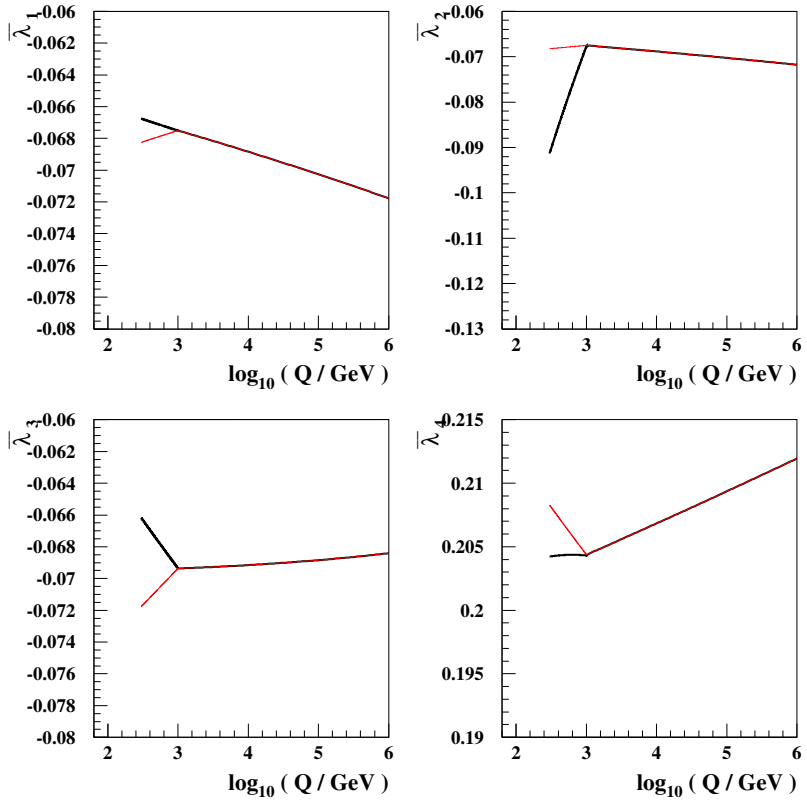

Figure 1. The black lines show the one-loop running of the 2HDM quartic couplings for $Q < 10^6\,\text{GeV}$, assuming $M_{H^\pm} = 300\,\text{GeV}$ and $\tan\beta = 5$. The other input parameters are given in eq. (4.1). The thin red lines show the running of $-(g^2 + g'^2)/8$, $-(g^2 - g'^2)/4$, and $g^2/2$ in the panels for $\bar{\lambda}_{1,2}$, $\bar{\lambda}_3$, and $\bar{\lambda}_4$, respectively.

the corresponding combinations of electroweak gauge couplings (red lines). Since there is a single SUSY-breaking scale of 1 TeV and hence a single threshold, the couplings are matched at this scale, and the red and black lines diverge as Q decreases from $M_S = 1\,\text{TeV}$ to $M_H = M_{H^\pm} = 300\,\text{GeV}$. Above M_S the RG evolution of the quartic couplings (black lines) are the same as those of the corresponding combinations of electroweak gauge couplings (red lines), i.e., the red and black lines lie on top of each other. This provides a non-trivial consistency check for the correctness of our results.

In the same context, it is important to comment that, for hierarchical scenarios with $\rho > 1$, where $\rho \equiv \max\left(\rho_{\tilde{Q},\tilde{U},\tilde{D},\tilde{L},\tilde{E}}\right)$, the proper matching conditions should be imposed at the highest soft SUSY-breaking scale $M'_S = \rho M_S$, rather than M_S. As an illustrative example, we consider another scenario with various different values for the soft SUSY breaking parameters:

$$\begin{aligned} \mu = 500\,\text{GeV}\,, \quad M_1 = 100\,\text{GeV}\,, \quad M_2 = 200\,\text{GeV}\,, \quad M_3 = 2\,i\,\text{TeV}\,, \\ m_{\tilde{Q}_3,\tilde{U}_3,\tilde{D}_3,\tilde{L}_3,\tilde{E}_3} = 10\,\text{TeV}\,, \quad A_{t,b,\tau} = 1\,i\,\text{TeV}\,, \quad \rho_{\tilde{Q},\tilde{U},\tilde{D},\tilde{L},\tilde{E}} = 10\,. \end{aligned} \tag{4.2}$$

JHEP02(2016)123

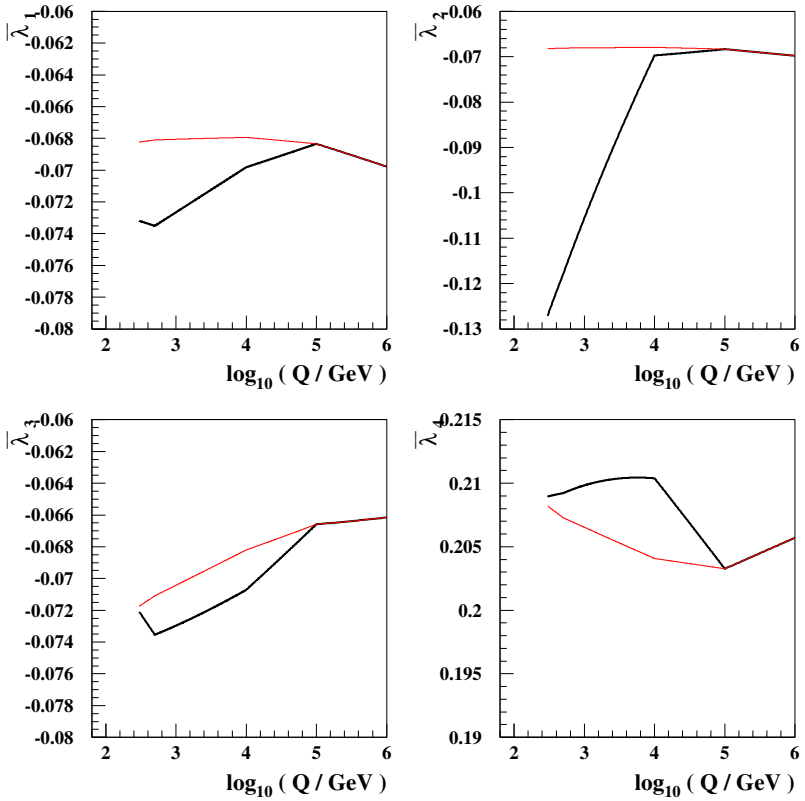

Figure 2. The same as in figure 1, but for an hierarchical scenario with $\rho = 10$ and input parameters given in eq. (4.2).

In this scenario, the matching conditions are imposed at the highest soft SUSY-breaking scale $M_S' = 10^5\,\text{GeV}$ instead of $M_S = 10^4\,\text{GeV}$, as illustrated in figure 2. We observe that the running between M_S and M_S' changes the size of the quartic couplings by an amount of $\sim 2\%$ for $\rho = 10$, which results in a less than 1 GeV increase in the mass prediction for the H_1 boson. Even though such changes may not appear too significant for scenarios with mass spectrum hierarchies of $\rho \lesssim 10$, they are nevertheless accurately described within our multi-threshold RG approach that we follow here for the computation of the Higgs-boson masses and mixing angles.

Next, we compare some results of `CPsuperH3.0` with the corresponding results of `CPsuperH2.3` in the MHMAX scenario [38, 39], where $X_t = \sqrt{6}M_S$ and $\mu = 200\,\text{GeV}$. In order to isolate the effects of the running in the range $M_H < Q < M_S$, where the effective 2HDM description is valid, we consider examples with $M_{H^\pm} \simeq m_t^{\text{pole}}$. Figure 3 compares calculations of the lightest Higgs mass M_{H_1}, and figure 4 shows results for the two heavier neutral Higgs bosons $H_{1,2}$, for $M_{H^\pm} = 180\,\text{GeV}$. In order to isolate the effects of the resummation of logarithms associated with the RG effects, we modified `CPsuperH2.3`, setting $m_t(m_t^{\text{pole}}) = 162.88\,\text{GeV}$ as obtained using eq. (3.4), instead of the value obtained from the one-loop relation between the pole and running masses: $m_t(m_t^{\text{pole}}) = m_t^{\text{pole}}/[1 + 4\alpha_s(m_t^{\text{pole}})/(3\pi)] \simeq 165.5\,\text{GeV}$, that was the standard value in `CPsuperH2.3`. The lower

JHEP02(2016)123

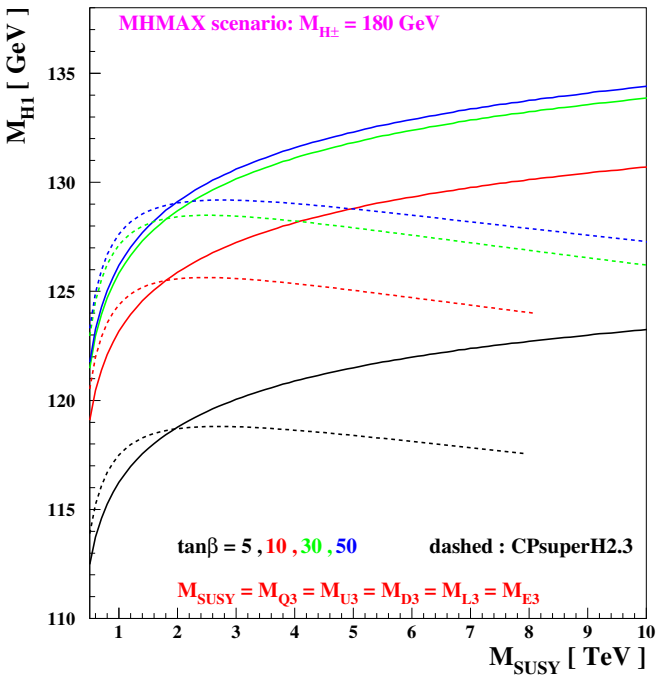

Figure 3. The lightest Higgs mass calculated in the MHMAX scenario using `CPsuperH3.0` (solid lines) and `CPsuperH2.3` (dashed lines) as functions of $M_S = M_{Q3} = M_{U3} = M_{D3} = M_{L3} = M_{E3}$ for $M_{H^\pm} = 180$ GeV, $\mu = 200\,\text{GeV}$ and various values of $\tan\beta$.

value of the running top quark mass we use is based on higher-order loop corrections to the relation between the pole and running masses [36, 37] and, as stressed before, it is used as the standard value for `CPsuperH3.0`.

From figure 3 we see that in the MHMAX scenario, the mass of the lightest Higgs boson calculated using `CPsuperH3.0` is $\sim 1\,\text{GeV}$ smaller than that obtained using `CPsuperH2.3` for $M_S = M_{\tilde{Q}_3} = M_{\tilde{U}_3} = M_{\tilde{D}_3} = M_{\tilde{L}_3} = M_{\tilde{E}_3} = 1\,\text{TeV}$.[3] This $\sim 1\,\text{GeV}$ difference may be attributed to the use of h_t^{2HDM} in `CPsuperH3.0` in the running to low energies. Namely, whereas in `CPsuperH2.3` the top Yukawa coupling appearing in $\lambda_2^{(1),(2)}$ given by eqs. (3.4) and (3.10) of ref. [14] includes the threshold corrections, we have not included these corrections in `CPsuperH3.0`. These Yukawa thresholds are still included in the relevant computation of the threshold corrections to the quartic couplings, which lead to the asymmetry between positive and negative values of $X_t = A_t - \mu^*/\tan\beta$ in the CP-conserving limit of the theory. This small difference between the `CPsuperH3.0` and `CPsuperH2.3` is rapidly compensated by RG effects and, as expected, the mass difference changes sign when $M_S \sim 2\,\text{TeV}$, and the new calculation of M_{H_1} is larger than the old one by $\sim 5\,\text{GeV}$ when $M_S \sim 8\,\text{TeV}$, the difference being only weakly dependent on $\tan\beta$. We do not show results for `CPsuperH2.3` at $\tan\beta = 5$ and 10 and $M_S > 8\,\text{TeV}$, since this program becomes unstable for that region of parameters.

[3] Here we ignore the small difference of M_S from that defined in eq. (3.1), but this difference is taken into account in all the numerical results presented in this work.

JHEP02(2016)123

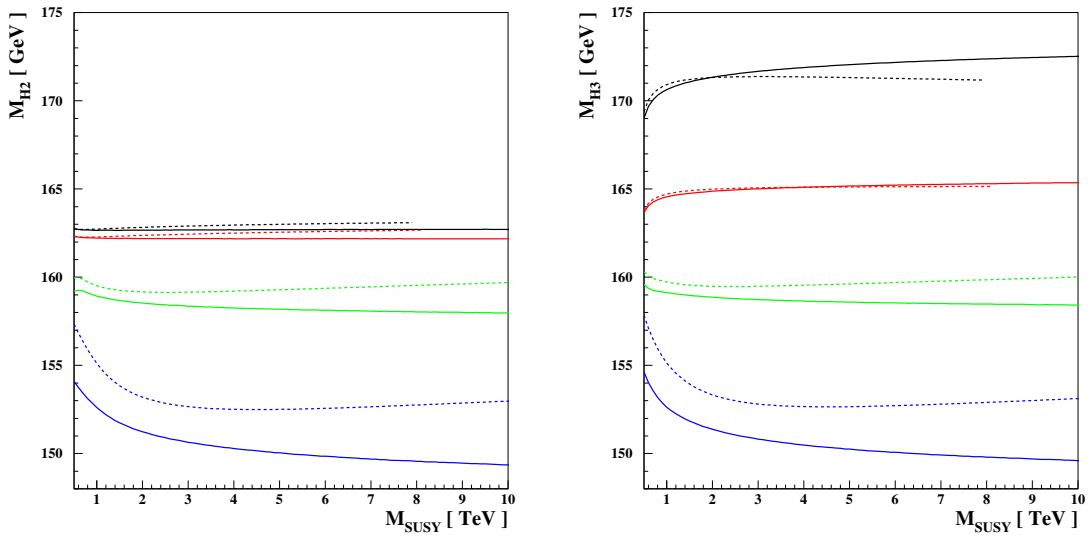

Figure 4. The two heavier neutral Higgs masses $M_{H_{2,3}}$ calculated in the MHMAX scenario using `CPsuperH3.0` (solid lines) and `CPsuperH2.3` (dashed lines), for the same parameter choices as in figure 3.

Figure 4 shows corresponding comparisons of the masses of the two heavier neutral Higgs bosons $M_{H_{2,3}}$ for the same parameter values. We see that the differences are very small for $\tan\beta = 5$ and 10, but increase for larger $\tan\beta$ and larger M_S, reaching $\sim 4\,\text{GeV}$ for $\tan\beta = 50$ and $M_S = 10\,\text{TeV}$.

Figure 5 shows another comparison of calculations of M_{H_1} made using `CPsuperH3.0` (solid lines) and `CPsuperH2.3` (dashed lines), this time as a function of X_t/M_S for $M_S = 1\,\text{TeV}$ (black lines), 2 TeV (red lines) and 4 TeV (blue lines). These calculations were made assuming $M_{H^\pm} = 180\,\text{GeV}$, $\mu = M_2 = 2M_1 = 200\,\text{GeV}$ and $\tan\beta = 20$. We see that the differences in M_{H_1} are again small, i.e., $\lesssim 1\,\text{GeV}$, for most values of X_t/M_S, though rising to $\sim 2\,\text{GeV}$ for $X_t/M_S \sim -2$. The results of `CPsuperH3.0` are in agreement with those obtained in ref. [33]. Figure 6 compares calculations of M_{H_1} made within `CPsuperH3.0` using the two-loop 2HDM RGEs (solid lines) and the one-loop 2HDM RGEs (dashed lines), again as a function of X_t/M_S for $M_S = 1\,\text{TeV}$ (black lines), 2 TeV (red lines) and 4 TeV (blue lines). We see that the full two-loop results are generally smaller than those in the one-loop approximation by $< 1\,\text{GeV}$, providing an encouraging estimate of their reliability.

Figure 7 shows some results from `CPsuperH3.0` for some larger values of M_S and $M_H = M_{H^\pm}$ where `CPsuperH2.3` would have been inapplicable. The left panel shows M_{H_1} for $M_{H^\pm} = M_S \leq 100\,\text{TeV}$ for two cases, $\tan\beta = 4$ and $X_t/M_S = \sqrt{6}$ (black line) and $\tan\beta = 20$ and $X_t/M_S = 0$ (red line) both for the case $\mu = M_2 = 2M_1 = 200\,\text{GeV}$ considered in figure 5. There is no 2HDM running effects in these plots, only the effects of SM running up to the common new physics threshold. Even allowing for an uncertainty of about 3 GeV in these calculations, values of $M_S = M_{H^\pm} > 15\,\text{TeV}$ lead to values of the lightest Higgs mass M_{H_1} that are incompatible with the measured values at the LHC, so the extension of the M_S axis to 100 TeV is largely for illustrative purposes.

JHEP02(2016)123

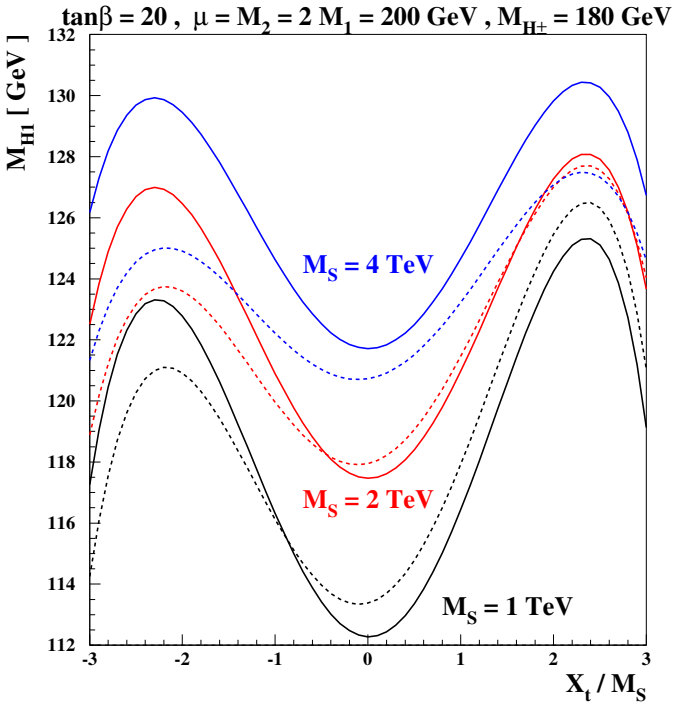

Figure 5. The lightest Higgs mass calculated as a function of X_t/M_S using `CPsuperH3.0` (solid lines) and `CPsuperH2.3` (dashed lines) for $M_{H^\pm} = 180\,\text{GeV}$, $\mu = M_2 = 2M_1 = 200\,\text{GeV}$ and $\tan\beta = 20$ for $M_S = 1\,\text{TeV}$ (black lines), 2 TeV (red lines) and 4 TeV (blue lines).

The right panel of figure 7 shows some other results for larger values of $M_{H^\pm}$ over the full range $[m_t, M_S]$ for $M_S = 1, 2$ and 4 TeV (black, red and blue lines, respectively) in the same two cases $X_t/M_S = \sqrt{6}$, $\tan\beta = 4$ and $X_t/M_S = 0$, $\tan\beta = 20$, considered previously, again with $\mu = M_2 = 2M_1 = 200\,\text{GeV}$. For these values of $\tan\beta$, the measured values of the Higgs mass is consistent with $M_S = 4\,\text{TeV}$ in the $X_t/M_S = \sqrt{6}$, $\tan\beta = 4$ case.[4]

5 CP-violating heavy Higgs scenarios

We now consider various CPX4LHC benchmark scenarios for showcasing the effect of CP violation in the MSSM heavy Higgs sector and their possible signatures. We assume a common CP-violating phase $\Phi_A = \arg(A_t) = \arg(A_b) = \arg(A_\tau)$, set

$$|A_{t,b,\tau}| \;=\; \mu \;=\; 2\,M_S\;, \tag{5.1}$$

with $M_2 = 2\,M_1 = 200$ GeV and $M_3 = 2$ TeV, and vary $\tan\beta$, $M_{H^\pm}$, and M_S. We do not include gaugino phases in this analysis, as they enter the Higgs sector only through the threshold corrections to the MSSM top-, bottom-, and tau-Yukawa couplings. Instead, we include the CP-conserving leading-log enhanced contributions due to gauginos to the self-energies $\Pi^{\pm,S,P}$. In our CPX4LHC scenarios, since we fix $M_2 = 2M_1 = 200$ GeV

[4]The results in the left and right panes of figure 7 should be compared to the ones in the lower-left frames of figures 1 and 2, and of figure 6 in ref. [35]

JHEP02(2016)123

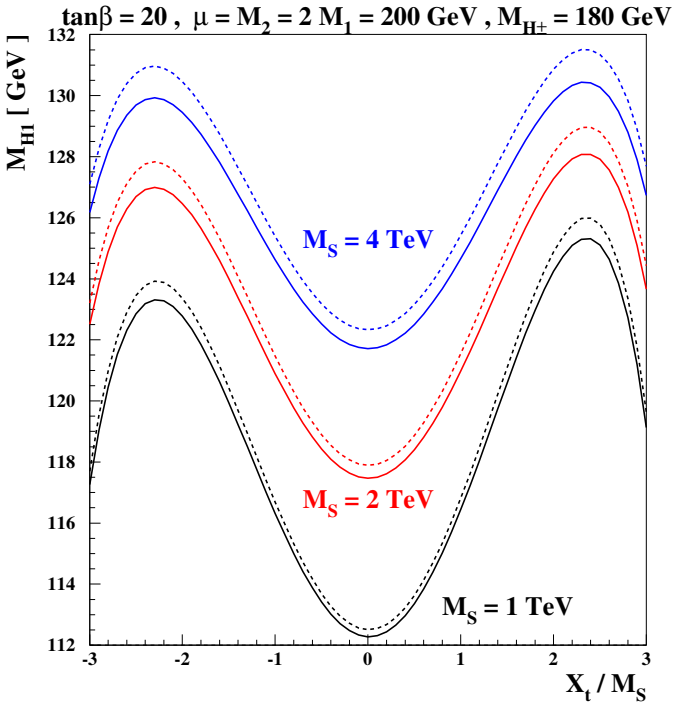

Figure 6. The lightest Higgs mass calculated as a function of X_t/M_S including (solid lines) and without including (dashed lines) the two-loop 2HDM contributions to the RGEs for $M_{H^\pm} = 180\,\text{GeV}$, $\mu = M_2 = 2M_1 = 200\,\text{GeV}$ and $\tan\beta = 20$ for $M_S = 1\,\text{TeV}$ (black lines), 2 TeV (red lines) and 4 TeV (blue lines).

and $M_3 = 2\,\text{TeV}$, and do not increase them as M_S increases, the gaugino phase effects are relatively insignificant.

We first present in figure 8 results for M_{H_1} as a function of Φ_A for the representative choices $M_{H^\pm} = 500\,\text{GeV}$, $M_S = 1, 2, 5, 10\,\text{TeV}$ and $\tan\beta = 5, 10, 30, 50$. The changes in M_{H_1} as Φ_A varies are small in general, namely $\lesssim 3\,\text{GeV}$ for $\tan\beta = 5$ and less for larger $\tan\beta$. Nevertheless, these variations are potentially significant, as there are parameter choices that would be excluded (in the sense of yielding values of M_{H_1} more than 3 GeV different from the measured value) for $\Phi_A = 0$ that would be allowed for $\Phi_A \neq 0$, e.g., $M_S = 5\,\text{TeV}$ and $\tan\beta = 5$. Conversely, there are cases where $\Phi_A = 0$ would be allowed, but $\Phi_A \neq 0$ would be disallowed, e.g., $M_S = 10\,\text{TeV}$ and $\tan\beta = 10$. The change in the lightest Higgs mass M_{H_1} at lower values of $\tan\beta$ can be understood from the change in the modulus of $X_t = A_t - \mu^*/\tan\beta$, which governs the one-loop threshold corrections to the low-energy Higgs quartic coupling. It reaches a maximum when $|X_t|/M_S \simeq 2.4$, and becomes less significant as $\tan\beta$ increases. In addition to this change, there are two-loop effects governed by the relative phase of A_t and M_3, which in the CP-conserving case tend to decrease (increase) M_{H_1} for negative (positive) values of $A_t M_3^*$, which explains why, for large values of $\tan\beta$, for which the variation of $|X_t|$ is small, the maximum value of M_{H_1} occurs for $\Phi(A_t) = 0$.

JHEP02(2016)123

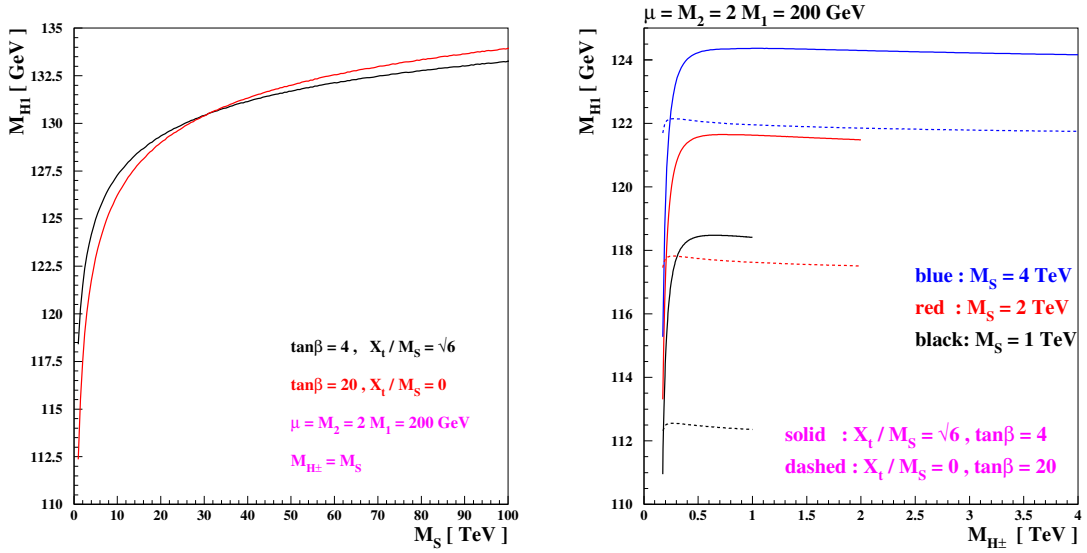

Figure 7. Left panel: halculations of M_{H_1} made using `CPsuperH3.0` for $M_{H^\pm} = M_S \leq 100\,\text{TeV}$, assuming $\tan\beta = 4$ and $X_t/M_S = \sqrt{6}$ (black line) and $\tan\beta = 20$ and $X_t/M_S = 0$ (red line) both for the case $\mu = M_2 = 2M_1 = 200\,\text{GeV}$. Right panel: calculations of M_{H_1} as a function of $m_{H^\pm}$ made using `CPsuperH3.0` over the range $M_{H^\pm} \in [m_t, M_S]$ for $M_S = 1, 2$ and $4\,\text{TeV}$ (black, red and blue lines, respectively), also for the two cases $X_t/M_S = \sqrt{6}$ and $\tan\beta = 4$ (solid lines) and $X_t/M_S = 0$ and $\tan\beta = 20$ (dashed lines) and $\mu = M_2 = 2M_1 = 200\,\text{GeV}$. These results can be compared with those of [35].

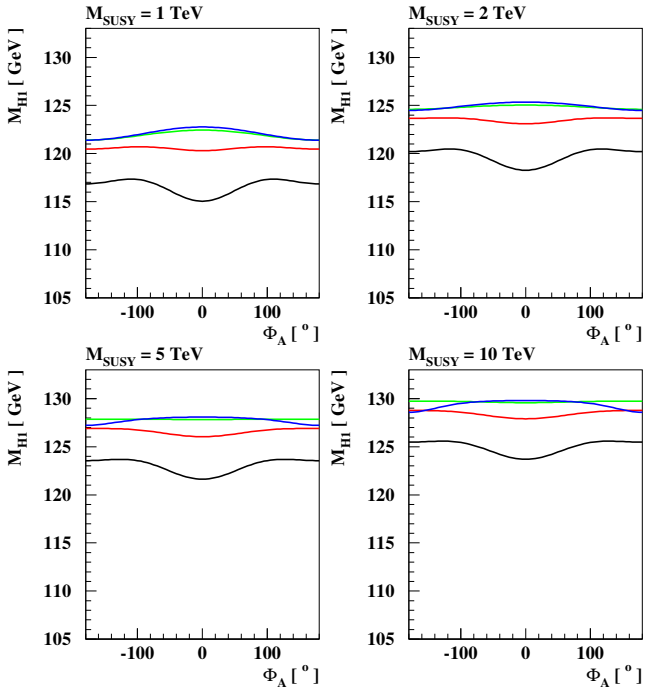

Figure 8. Values of M_{H_1} in CP-violating scenarios for $M_{H^\pm} = 500\,\text{GeV}$ and $M_S = 1\,\text{TeV}$ (upper left), $M_S = 2\,\text{TeV}$ (upper right), $M_S = 5\,\text{TeV}$ (lower left), $M_S = 10\,\text{TeV}$ (lower right). The black, red, green and blue lines are for $\tan\beta = 5, 10, 30$ and 50, respectively.

JHEP02(2016)123

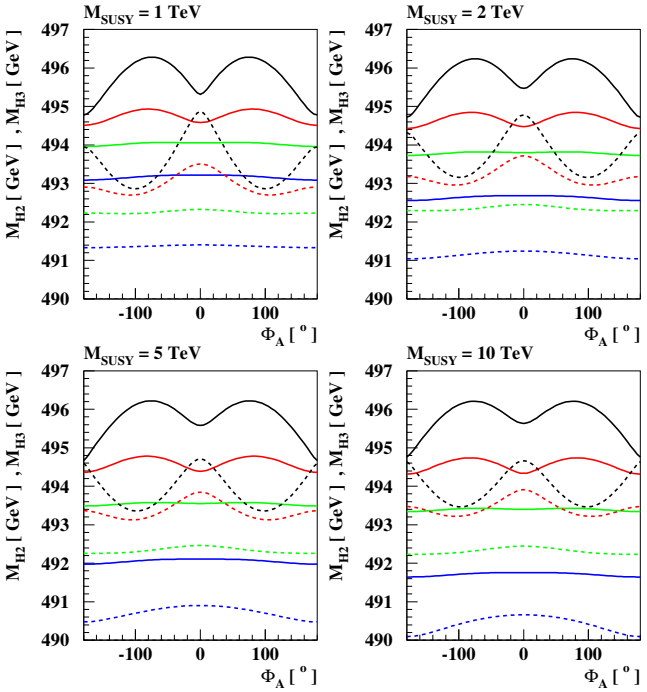

Figure 9. Values of M_{H_3} (solid lines) and M_{H_2} (dashed lines) in CP-violating scenarios for $M_{H^\pm} = 500\,\text{GeV}$ and $M_S = 1\,\text{TeV}$ (upper left), $M_S = 2\,\text{TeV}$ (upper right), $M_S = 5\,\text{TeV}$ (lower left), $M_S = 10\,\text{TeV}$ (lower right). The black, red, green and blue lines are for $\tan\beta = 5, 10, 30$ and 50, respectively.

Figure 9 displays the corresponding values of M_{H_3} (solid lines) and M_{H_2} (dashed lines) for $M_{H^\pm} = 500\,\text{GeV}$ and the same values of M_S and $\tan\beta$ as in figure 8. We see that in general the mass difference $M_{H_3} - M_{H_2}$ is minimized in the CP-conserving cases $\Phi_A = 0, 180°$, where it is $\lesssim 1\,\text{GeV}$, and maximized when $\Phi_A = \pm 90°$, where it may be $\sim 3\,\text{GeV}$. Thus, a measurement of the $H_3 - H_2$ mass difference could be an indirect diagnostic tool indicative of CP violation, even if the latter is not directly observable.

We now consider predictions for two direct measures of CP violation in the Higgs mass eigenstates H_i (with $i = 1, 2, 3$):

$$\langle \phi_1 a : H_i \rangle \equiv \frac{2 O_{\phi_1 i} O_{ai}}{O_{\phi_1 i}^2 + O_{ai}^2}\,, \qquad \langle \phi_2 a : H_i \rangle \equiv \frac{2 O_{\phi_2 i} O_{ai}}{O_{\phi_2 i}^2 + O_{ai}^2}\,, \tag{5.2}$$

which characterize the mixtures between the CP-odd state a and the CP-even states $\phi_{1,2}$. For instance, such CP-violating expressions occur when studying CP violation in Higgs-boson decays to fermions [23, 40]. For a recent analysis of CP violation in the decays $H_{1,2,3} \to \tau^+\tau^-$, see [41]. Figure 10 displays values of $\langle \phi_1 a : H_1 \rangle$ for the lightest neutral mass eigenstate H_1, for the same scenarios $M_{H^\pm} = 500\,\text{GeV}$, $M_S = 1, 2, 5, 10\,\text{TeV}$ and $\tan\beta = 5, 10, 30$ and 50 discussed previously. We see that the values increase for smaller values of M_S and larger values of $\tan\beta$, and that values as large as ± 0.22 are possible for $\tan\beta = 50$ and $M_S = 1\,\text{TeV}$. Even larger values would be possible for smaller values of $M_{H^\pm}$ and M_S.

JHEP02(2016)123

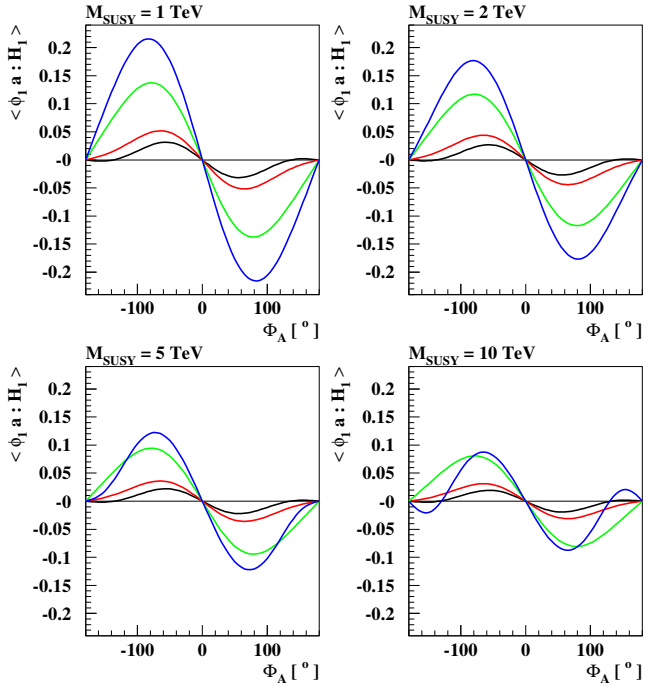

Figure 10. The CP mixing quantity $\frac{2O_{\phi_1 1}O_{a1}}{O^2_{\phi_1 1}+O^2_{a1}}$ for the lightest mass eigenstate H_1 in scenarios with $M_{H^\pm} = 500\,\text{GeV}$ and $M_S = 1\,\text{TeV}$ (upper left), $M_S = 2\,\text{TeV}$ (upper right), $M_S = 5\,\text{TeV}$ (lower left), $M_S = 10\,\text{TeV}$ (lower right). The black, red, green and blue lines are for $\tan\beta = 5, 10, 30$ and 50, respectively.

Figure 11 shows values of the other mixing coefficient $\langle \phi_2 a : H_1 \rangle$ for H_1 in the same set of CP-violating scenarios. This coefficient takes values $\lesssim 0.007$ for $M_{H^\pm} = 500\,\text{GeV}$, $M_S = 1\,\text{TeV}$ and $\tan\beta = 5$, decreasing for larger $M_{H^\pm}$, M_S and $\tan\beta$.

Similar results for the second mass eigenstate H_2 are shown in figures 12 and 13, and for the third mass eigenstate H_3 in figures 14 and 15. We see here that the mixing quantities (5.2) can be *much larger* for the heavy mass eigenstates $H_{2,3}$ than for the lightest mass eigenstate H_1, attaining unity for many of the values of M_S and $\tan\beta$ studied. This suggests, *a priori*, that the prospects for observing CP violation would be enhanced for the heavier Higgs mass eigenstates H_2 and H_3.

These results illustrate the possible non-decoupling of CP-violating effects in the heavier neutral Higgs bosons $H_{2,3}$ for large values of $M_{H^\pm}$ and M_S, whereas the corresponding quantities for the lightest neutral Higgs mass eigenstate are expected to decouple. This is seen explicitly in figures 16, where we display the absolute values of $\langle \phi_1 a : H_i \rangle$ (left) and $\langle \phi_2 a : H_i \rangle$ (right) for $M_S = 10\,\text{TeV}$ and $\Phi_A = 10^\circ$ as functions of $M_{H^\pm}$ for the same values of $\tan\beta$ considered previously. The corresponding results for $\Phi_A = 60^\circ$ are shown in figure 17. In the case of H_1, we see that the mixing quantities $\to 0$ at large $M_{H^\pm}$, as expected, whereas in general the corresponding coefficients for the heavy neutral Higgs mass eigenstates $H_{2,3}$ do not vanish, and retain large values even for very large $M_{H^\pm}$.

JHEP02(2016)123

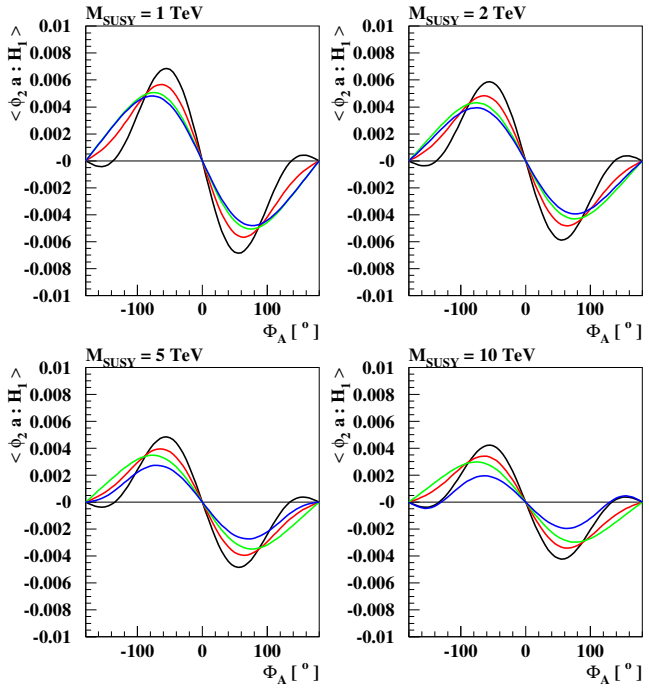

Figure 11. As in figure 10, but showing the CP mixing quantity $\frac{2O_{\phi_2 1}O_{a1}}{O^2_{\phi_2 1}+O^2_{a1}}$ for the lightest mass eigenstate H_1.

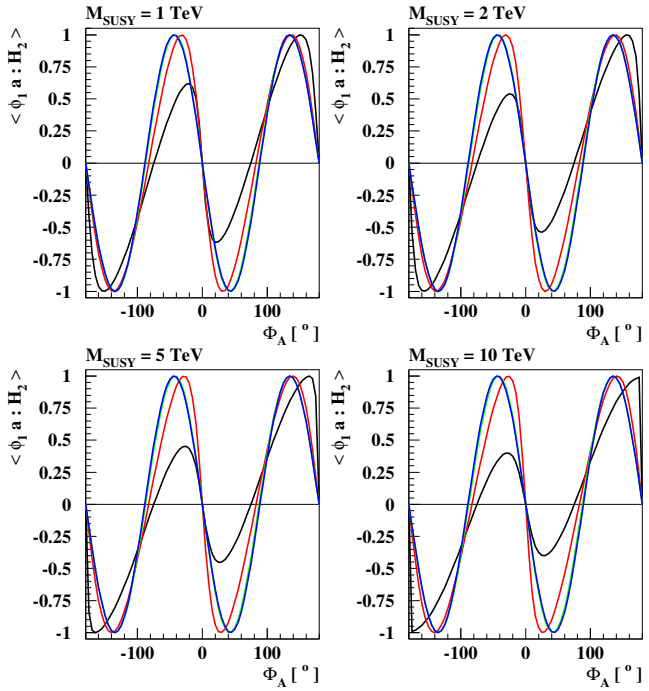

Figure 12. As in figure 10, but showing the CP mixing quantity $\frac{2O_{\phi_1 2}O_{a2}}{O^2_{\phi_1 2}+O^2_{a1}}$ for the second mass eigenstate H_2.

JHEP02(2016)123

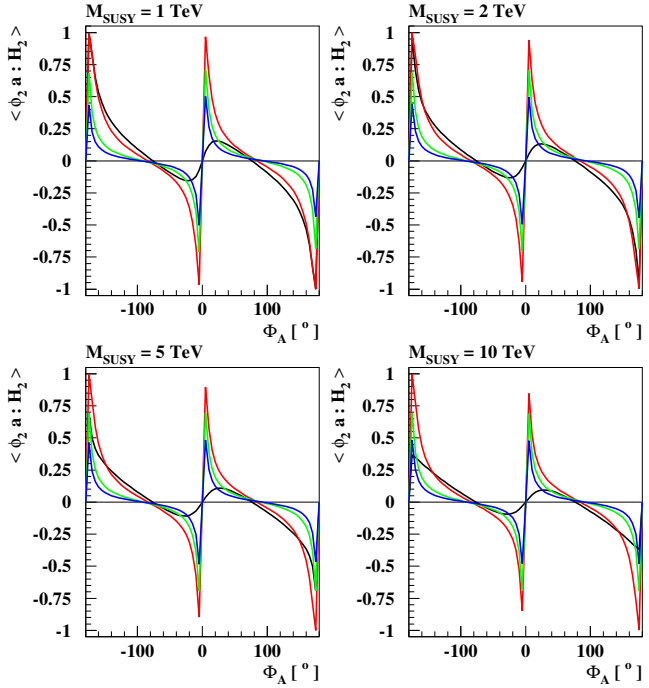

Figure 13. As in figure 10, but showing the CP mixing quantity $\frac{2O_{\phi_2 2}O_{a2}}{O^2_{\phi_2 2}+O^2_{a1}}$ for the second mass eigenstate H_2.

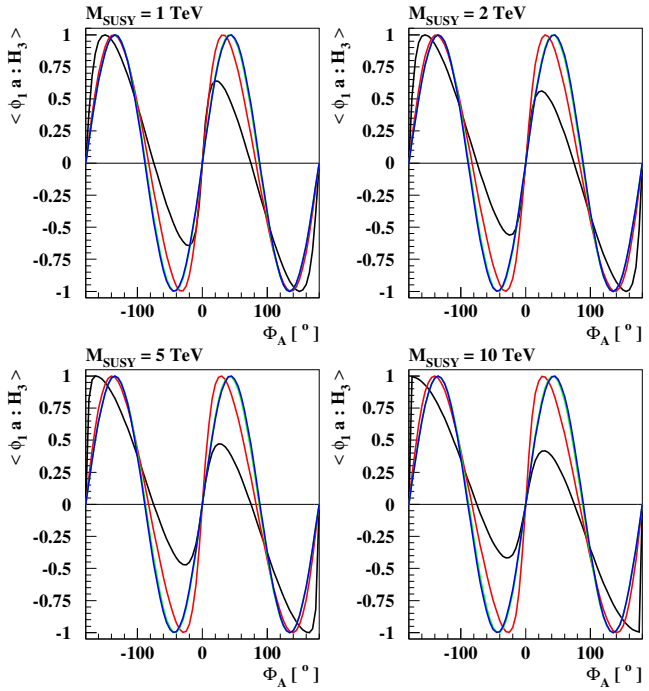

Figure 14. As in figure 10, but showing the CP mixing quantity $\frac{2O_{\phi_1 3}O_{a3}}{O^2_{\phi_1 3}+O^2_{a3}}$ for the third mass eigenstate H_3.

JHEP02(2016)123

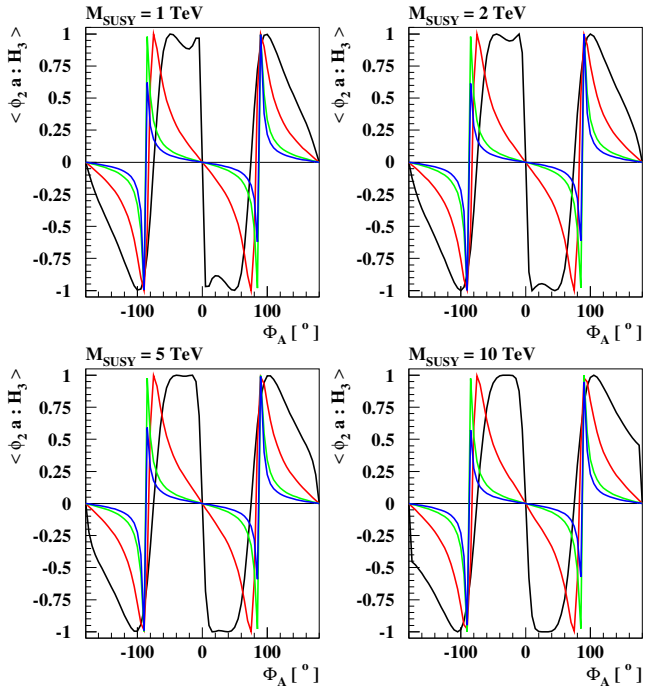

Figure 15. As in figure 10, but showing the CP mixing quantity $\frac{2O_{\phi_2 3}O_{a3}}{O^2_{\phi_2 3}+O^2_{a3}}$ for the third mass eigenstate H_3.

Thus, large CP-violating effects in the couplings of these states are a robust signature of the CP-violating scenarios discussed in this paper.

6 Conclusions

We present new MSSM scenarios with explicit CP violation that contain heavy Higgs bosons in the few to several hundred GeV range and are consistent with constraints from Run I of the LHC. The scenarios suggested here are similar in spirit to the CPX scenarios previously proposed , and have phenomenological implications that can be tested during Run II of the LHC. In light of this, we call them CPX4LHC benchmark scenarios.

In this work we explicitly demonstrate that, although CP violation and other new-physics effects decouple from the lightest Higgs boson sector for sufficiently large charged Higgs boson masses and soft SUSY-breaking scales M_S, they can still be significant in the MSSM heavy Higgs boson sector. Large masses of the supersymmetric particles also help to maintain agreement with limits on EDMs and other low-energy observables. We consider scenarios in which the charged Higgs bosons $H^\pm$ and the two heavier neutral Higgs bosons $H_{2,3}$ could be much lighter than all third generation supersymmetric scalar fermions, which are assumed to have masses $M_S \gtrsim 2\,\text{TeV}$. In light of this possibility, we have revisited previous calculations by considering improved matching and renormalization group (RG) effects, specifically including two-loop RG effects in the two-Higgs-doublet model (2HDM) that is effective between the heavy Higgs scale $M_{H^\pm}$ and the SUSY scale M_S.

JHEP02(2016)123

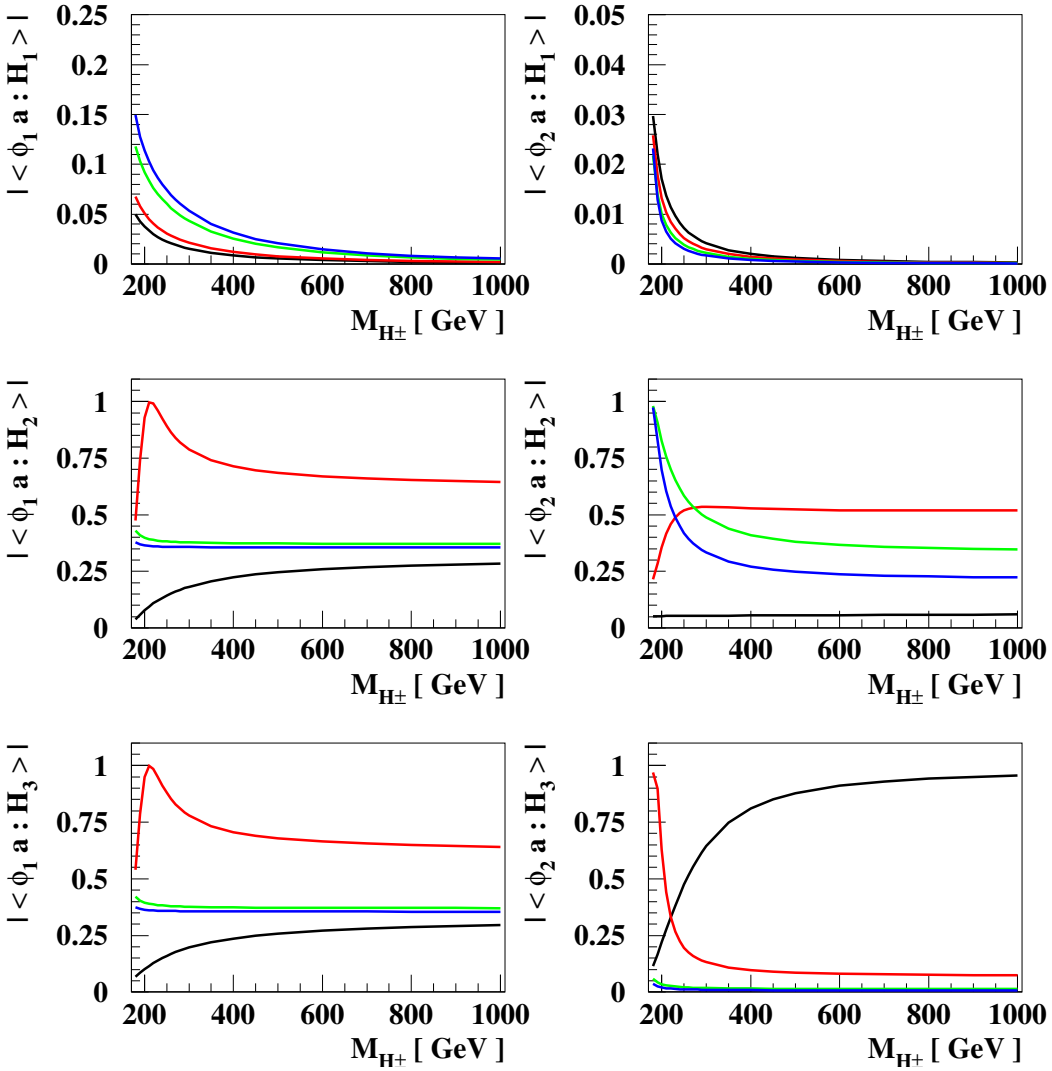

Figure 16. The magnitudes of the mixing quantities $|\langle\phi_1 a : H_i\rangle|$ (left) and $|\langle\phi_2 a : H_i\rangle|$ (right), defined in (5.2), as functions of $M_{H^\pm}$ for $M_S = 10\,\text{TeV}$ and $\Phi_A = 10°$. The black, red, green and blue lines are for $\tan\beta = 5, 10, 30$ and 50, respectively.

We compare our new results with those obtained with the previous code version `CPsuperH2.3`. We also discuss the specific CPX4LHC benchmark scenarios relevant for the analysis of Higgs physics at the LHC, with particular emphasis on the masses of the heavier neutral Higgs bosons $H_{2,3}$ and on the CP-violating effects they may manifest. These offer interesting prospects for future runs of the LHC and future colliders.

All the improvements discussed in this study are being incorporated in a new version of the public code `CPsuperH`, called `CPsuperH3.0`. The numerical results presented here have been obtained by means of a preliminary β-version of this code. The detailed features of `CPsuperH3.0` will be fully described in an upcoming release note.[5]

[5]The current β-version is available upon request to J. S. Lee.

JHEP02(2016)123

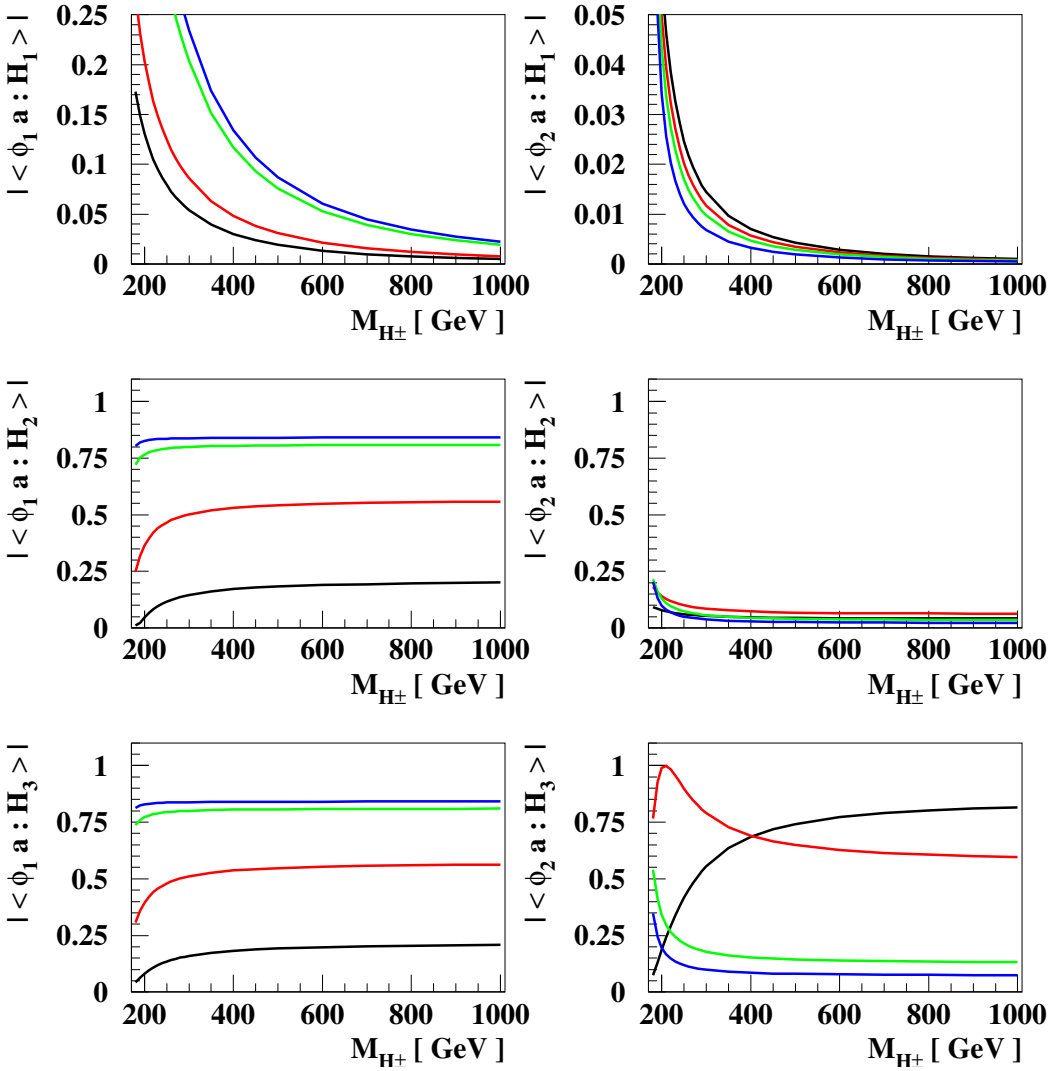

Figure 17. As in figure 16 but for for $M_S = 10\,\text{TeV}$ and $\Phi_A = 60°$.

Acknowledgments

Fermilab is operated by Fermi Research Alliance, LLC under Contract No. DE-AC02-07CH11359 with the U.S. Department of Energy, and University of Chicago is supported in part by U.S. Department of Energy grant number DE-FG02-13ER41958. The work of J.E. is supported in part by the London Centre for Terauniverse Studies (LCTS), using funding from the European Research Council via the Advanced Investigator Grant 267352, and in part by STFC (U.K.) via the research grant ST/L000326/1. The work of J.S.L. is supported by the National Research Foundation of Korea (NRF) grant (No. 2013R1A2A2A01015406). The work of A.P. is supported by the Lancaster-Manchester-Sheffield Consortium for Fundamental Physics under STFC grant ST/L000520/1. Work at ANL is supported in part by the U.S. Department of Energy under Contract No. DE-

JHEP02(2016)123

AC02-06CH11357. M.C. and C.W. thank for its hospitality the Aspen Center for Physics, which is supported by the National Science Foundation under Grant No. PHYS-1066293.

A Renormalization group equations and threshold corrections

In the appendices that follow, we present the relevant Renormalization Group Equations (RGEs) that are applicable above the three typical thresholds: (i) the top-quark mass m_t, (ii) the heavy Higgs mass $M_H \equiv M_{H^+}$, and (iii) the soft SUSY-breaking scale M_S.

It is convenient to write the RGEs in the form

$$\frac{\mathrm{d}c}{\mathrm{d}t} \;=\; \sum_{n=1} \kappa^n \, \beta_c^{(n)} \;,$$

where c stands for any kinematic parameter, such as quartic, gauge and Yukawa couplings, anomalous dimensions, and $\tan\beta$. In addition, we use the abbreviations: $t \equiv \ln Q$ and $\kappa = 1/(4\pi)^2$.

A.1 SM RGEs

For scales of Q, for which $M_{H_1} \sim m_t < Q < M_H$, one needs to consider the RGEs of the SM. To properly take into consideration intermediate particle threshold effects, we introduce the short-hand notation for the step function

$$\Theta_X \;\equiv\; \begin{cases} 1 \text{ for } \; Q \geq M_X \,, \\ 0 \text{ for } \; Q < M_X \,. \end{cases}$$

Upon neglecting the Yukawa couplings of the first two generations of quarks and leptons, the one-loop SM RGEs that we use [35, 42] read:

$$\begin{aligned}
\beta_\lambda^{(1)} \;=\; & 12\lambda^2 + 4\lambda\left(3y_t^2 + 3y_b^2 + y_\tau^2\right) - 4\left(3y_t^4 + 3y_b^4 + y_\tau^4\right) \\
& -9\lambda\left(g^2 + \frac{1}{3}g'^2\right) + \frac{9}{4}\left(g^4 + \frac{2}{3}g'^2 g^2 + \frac{1}{3}g'^4\right) \\
& + \left(6\lambda g^2 - 5g^4 + 8g^4 s_\beta^2 c_\beta^2\right)\Theta_{\widetilde{H}}\Theta_{\widetilde{W}} \\
& -2g^2 g'^2 \Theta_{\widetilde{H}}\Theta_{\widetilde{W}}\Theta_{\widetilde{B}} + \left(2\lambda g'^2 - g'^4\right)\Theta_{\widetilde{H}}\Theta_{\widetilde{B}} \,, \qquad \text{(A.1)} \\
\beta_\lambda^{(2)} \;=\; & -78\lambda^3 - 72\lambda^2 y_t^2 + 80\lambda g_s^2 y_t^2 - 3\lambda y_t^4 - 64 g_s^2 y_t^4 + 60 y_t^6 \,, \qquad \text{(A.2)} \\
\beta_\lambda^{(3)} \;=\; & \frac{\lambda^3}{2}\left(6011.35\frac{\lambda}{2} + 873 y_t^2\right) + \lambda^2 y_t^2\left(1768.26 y_t^2 + 160.77 g_s^2\right) \\
& +2\lambda y_t^2\left(-223.382 y_t^4 - 662.866 g_s^2 y_t^2 + 356.968 g_s^4\right) \\
& +4 y_t^4\left(-243.149 y_t^4 + 250.494 g_s^2 y_t^2 - 50.201 g_s^4\right) \,, \qquad \text{(A.3)} \\
\beta_{g_s}^{(1)} \;=\; & -g_s^3\left[11 - \frac{2}{3}N_f\right] \,, \qquad \text{(A.4)} \\
\beta_{g_s}^{(2)} \;=\; & -g_s^3\left[\left(102 - \frac{38}{3}N_f\right)g_s^2 - \frac{3}{4}N_f g^2 - \frac{11}{36}N_f g'^2 + 2y_t^2 + 2y_b^2\right] \,, \qquad \text{(A.5)} \\
\beta_{y_t}^{(1)} \;=\; & y_t\left[\frac{9}{2}y_t^2 + \frac{3}{2}y_b^2 + y_\tau^2 - 8g_s^2 - \frac{9}{4}g^2 - \frac{17}{12}g'^2\right] \\
& +\frac{3}{2}y_t g^2 \Theta_{\widetilde{H}}\Theta_{\widetilde{W}} + \frac{1}{2}y_t g'^2 \Theta_{\widetilde{H}}\Theta_{\widetilde{B}} \,, \qquad \text{(A.6)}
\end{aligned}$$

$$\beta_{y_t}^{(2)} = y_t\left[\frac{3}{2}\lambda^2 - 6\lambda y_t^2 - \left(\frac{404}{3} - \frac{40}{9}N_f\right)g_s^4 + 36g_s^2y_t^2 - 12y_t^4\right], \tag{A.7}$$

$$\begin{aligned}\beta_{y_t}^{(3)} = y_t\Big[&-\frac{9}{2}\lambda^3 + \frac{15}{16}\lambda^2y_t^2 + \lambda y_t^2\left(99y_t^2 + 8g_s^2\right)\\ &+58.6028y_t^6 - 157y_t^4g_s^2 + 363.764y_t^2g_s^4 - 619.35g_s^6\Big],\end{aligned} \tag{A.8}$$

$$\beta_{y_b}^{(1)} = y_b\left[\frac{3}{2}y_t^2 + \frac{9}{2}y_b^2 + y_\tau^2 - 8g_s^2 - \frac{9}{4}g^2 - \frac{5}{12}g'^2\right], \tag{A.9}$$

$$\beta_{y_\tau}^{(1)} = y_\tau\left[3y_t^2 + 3y_b^2 + \frac{5}{2}y_\tau^2 - \frac{9}{4}g^2 - \frac{45}{12}g'^2\right], \tag{A.10}$$

$$\begin{aligned}\beta_{g'}^{(1)} &= \left(\frac{2}{3}N_f + \frac{1}{10}\right)\frac{5}{3}g'^3,\\ \beta_{g'}^{(2)} &= \left(\frac{22}{9}N_fg_s^2 - \frac{17}{6}y_t^2\right)g'^3,\\ \beta_g^{(1)} &= \left(-\frac{22}{3} + \frac{2}{3}N_f + \frac{1}{6}\right)g^3,\\ \beta_g^{(2)} &= \left(2N_fg_s^2 - \frac{3}{2}y_t^2\right)g^3,\end{aligned} \tag{A.11}$$

$$\gamma^{(1)} = \frac{9}{4}\left(g^2 + \frac{1}{3}g'^2\right) - \left(3y_t^2 + 3y_b^2 + y_\tau^2\right). \tag{A.12}$$

A.2 One-loop 2HDM RGEs

For RG scales Q between M_H and M_S, the effective theory becomes a general 2HDM, whilst for $Q > M_S$ the theory becomes fully supersymmetric and the quartic couplings $\lambda_{5,6,7}$ do not run. Here, we give the RGEs of the general 2HDM at the one-loop level, and relegate to appendix A.3 the presentation of the two-loop results.

As before, we neglect the Yukawa couplings of the first two generations of quarks and leptons, and note that in addition to the change of normalizations given in (2.5), we use $t = \ln(Q)$ instead of $\ln(Q^2)$ as used in ref. [31]. Thus, adapting the results of [31], the one-loop 2HDM RGEs may be listed as follows:

$$\begin{aligned}\beta_{\lambda_1}^{(1)} = &-\left\{24\lambda_1^2 + \lambda_3^2 + (\lambda_3+\lambda_4)^2 + 4\lambda_5^2 + 12\lambda_6^2 + \frac{3}{8}\left[2g^4 + \left(g^2+g'^2\right)^2\right]\right\}\Theta_Z\\ &-N_C\Bigg\{-2h_b^4\Theta_Z + \left(h_b^2 - \frac{1}{4}g'^2Y_D\right)^2\Theta_{\widetilde{D}_3} + \left(\frac{1}{4}g'^2Y_U\right)^2\Theta_{\widetilde{U}_3}\\ &+\left[h_b^4 - \frac{1}{2}h_b^2\left(g'^2Y_Q + g^2\right) + \frac{1}{8}\left(g^4 + g'^4Y_Q^2\right)\right]\Theta_{\widetilde{Q}_3}\Bigg\}\\ &-N_C\sum_{i=1}^{2}\left\{\left(\frac{1}{4}g'^2Y_D\right)^2\Theta_{\widetilde{D}_i} + \left(\frac{1}{4}g'^2Y_U\right)^2\Theta_{\widetilde{U}_i} + \frac{1}{8}\left(g^4 + g'^4Y_Q^2\right)\Theta_{\widetilde{Q}_i}\right\}\\ &-\left\{-2h_\tau^4\Theta_Z + \left(h_\tau^2 - \frac{1}{4}g'^2Y_E\right)^2\Theta_{\widetilde{E}_3} + \left[h_\tau^4 - \frac{1}{2}h_\tau^2\left(g'^2Y_L + g^2\right) + \frac{1}{8}\left(g^4 + g'^4Y_L^2\right)\right]\Theta_{\widetilde{L}_3}\right\}\end{aligned}$$

JHEP02(2016)123

$$
\begin{aligned}
&-\sum_{i=1}^{2}\left\{\left(\frac{1}{4}g'^2Y_E\right)^2\Theta_{\widetilde{E}_i}+\frac{1}{8}\left(g^4+g'^4Y_L^2\right)\Theta_{\widetilde{L}_i}\right\}\\
&+\frac{5}{2}g^4\Theta_{\widetilde{H}}\Theta_{\widetilde{W}}+g'^2g^2\Theta_{\widetilde{H}}\Theta_{\widetilde{W}}\Theta_{\widetilde{B}}+\frac{1}{2}g'^4\Theta_{\widetilde{H}}\Theta_{\widetilde{B}}-4\lambda_1\gamma_1^{(1)}\,, \qquad \text{(A.13)}
\end{aligned}
$$

where $N_C=3$, $Y_Q=1/3$, $Y_U=-4/3$, $Y_D=2/3$, $Y_L=-1$, $Y_E=2$, and

$$
\begin{aligned}
\beta_{\lambda_2}^{(1)} =& -\left\{24\lambda_2^2+\lambda_3^2+(\lambda_3+\lambda_4)^2+4\lambda_5^2+12\lambda_6^2+\frac{3}{8}\left[2g^4+\left(g^2+g'^2\right)^2\right]\right\}\Theta_Z\\
&-N_C\Bigg\{-2h_t^4\Theta_t\Theta_Z+\left(\frac{1}{4}g'^2Y_D\right)^2\Theta_{\widetilde{D}_3}+\left(h_t^2+\frac{1}{4}g'^2Y_U\right)^2\Theta_{\widetilde{U}_3}\\
&+\left[h_t^4+\frac{1}{2}h_t^2\left(g'^2Y_Q-g^2\right)+\frac{1}{8}\left(g^4+g'^4Y_Q^2\right)\right]\Theta_{\widetilde{Q}_3}\Bigg\}\\
&-N_C\sum_{i=1}^{2}\left\{\left(\frac{1}{4}g'^2Y_D\right)^2\Theta_{\widetilde{D}_i}+\left(\frac{1}{4}g'^2Y_U\right)^2\Theta_{\widetilde{U}_i}+\frac{1}{8}\left(g^4+g'^4Y_Q^2\right)\Theta_{\widetilde{Q}_i}\right\}\\
&-\sum_{i=1}^{3}\left\{\left(\frac{1}{4}g'^2Y_E\right)^2\Theta_{\widetilde{E}_i}+\frac{1}{8}\left(g^4+g'^4Y_L^2\right)\Theta_{\widetilde{L}_i}\right\}\\
&+\frac{5}{2}g^4\Theta_{\widetilde{H}}\Theta_{\widetilde{W}}+g'^2g^2\Theta_{\widetilde{H}}\Theta_{\widetilde{W}}\Theta_{\widetilde{B}}+\frac{1}{2}g'^4\Theta_{\widetilde{H}}\Theta_{\widetilde{B}}-4\lambda_2\gamma_2^{(1)}\,, \qquad \text{(A.14)}\\
\beta_{\lambda_3}^{(1)} =& -2\Bigg\{2(\lambda_1+\lambda_2)(3\lambda_3+\lambda_4)+2\lambda_3^2+\lambda_4^2+4\lambda_5^2+2\lambda_6^2+2\lambda_7^2+8\lambda_6\lambda_7\\
&+\frac{3}{8}\left[2g^4+\left(g^2-g'^2\right)^2\right]\Bigg\}\Theta_Z\\
&-2N_C\Bigg\{-2h_t^2h_b^2\Theta_t\Theta_Z+\frac{1}{4}g'^2Y_D\left(h_b^2-\frac{1}{4}g'^2Y_D\right)\Theta_{\widetilde{D}_3}\\
&-\frac{1}{4}g'^2Y_U\left(h_t^2+\frac{1}{4}g'^2Y_U\right)\Theta_{\widetilde{U}_3}+h_t^2h_b^2\Theta_{\widetilde{U}_3}\Theta_{\widetilde{D}_3}\\
&+\left[h_t^2h_b^2-\frac{1}{4}h_t^2\left(g'^2Y_Q+g^2\right)+\frac{1}{4}h_b^2\left(g'^2Y_Q-g^2\right)+\frac{1}{8}\left(g^4-g'^4Y_Q^2\right)\right]\Theta_{\widetilde{Q}_3}\Bigg\}\\
&-2N_C\sum_{i=1}^{2}\left\{-\left(\frac{1}{4}g'^2Y_D\right)^2\Theta_{\widetilde{D}_i}-\left(\frac{1}{4}g'^2Y_U\right)^2\Theta_{\widetilde{U}_i}+\frac{1}{8}\left(g^4-g'^4Y_Q^2\right)\Theta_{\widetilde{Q}_i}\right\}\\
&-2\left\{\frac{1}{4}g'^2Y_E\left(h_\tau^2-\frac{1}{4}g'^2Y_E\right)\Theta_{\widetilde{E}_3}+\left[\frac{1}{4}h_\tau^2\left(g'^2Y_L-g^2\right)+\frac{1}{8}\left(g^4-g'^4Y_L^2\right)\right]\Theta_{\widetilde{L}_3}\right\}\\
&-2\sum_{i=1}^{2}\left\{-\left(\frac{1}{4}g'^2Y_E\right)^2\Theta_{\widetilde{E}_i}+\frac{1}{8}\left(g^4-g'^4Y_L^2\right)\Theta_{\widetilde{L}_i}\right\}\\
&+5g^4\Theta_{\widetilde{W}}\Theta_{\widetilde{H}}-2g'^2g^2\Theta_{\widetilde{W}}\Theta_{\widetilde{B}}\Theta_{\widetilde{H}}+g'^4\Theta_{\widetilde{B}}\Theta_{\widetilde{H}}-2\lambda_3\left(\gamma_1^{(1)}+\gamma_2^{(1)}\right), \qquad \text{(A.15)}
\end{aligned}
$$

JHEP02(2016)123

$$\beta^{(1)}_{\lambda_4} = -2\left[\lambda_4\left(2\lambda_1+2\lambda_2+4\lambda_3+2\lambda_4\right)+16\lambda_5^2+5\lambda_6^2+5\lambda_7^2+2\lambda_6\lambda_7+\frac{3}{2}g^2g'^2\right]\Theta_Z$$
$$-2N_C\left\{2h_t^2h_b^2\Theta_t\Theta_Z-h_t^2h_b^2\Theta_{\widetilde{U}_3}\Theta_{\widetilde{D}_3}-\left(h_t^2-\frac{1}{2}g^2\right)\left(h_b^2-\frac{1}{2}g^2\right)\Theta_{\widetilde{Q}_3}\right\}$$
$$+2N_C\sum_{i=1}^{2}\left(\frac{1}{2}g^2\right)^2\Theta_{\widetilde{Q}_i}-g^2\left(h_\tau^2-\frac{1}{2}g^2\right)\Theta_{\widetilde{L}_3}+\sum_{i=1}^{2}\frac{1}{2}g^4\Theta_{\widetilde{L}_i}$$
$$-4g^4\Theta_{\widetilde{W}}\Theta_{\widetilde{H}}+4g'^2g^2\Theta_{\widetilde{W}}\Theta_{\widetilde{B}}\Theta_{\widetilde{H}}-2\lambda_4\left(\gamma_1^{(1)}+\gamma_2^{(1)}\right), \tag{A.16}$$

$$\beta^{(1)}_{\lambda_5} = -\left[2\lambda_5(2\lambda_1+2\lambda_2+4\lambda_3+6\lambda_4)+5\left(\lambda_6^2+\lambda_7^2\right)+2\lambda_6\lambda_7\right]\Theta_Z-2\lambda_5\left(\gamma_1^{(1)}+\gamma_2^{(1)}\right), \tag{A.17}$$

$$\beta^{(1)}_{\lambda_6} = -2\left[\lambda_6\left(12\lambda_1+3\lambda_3+4\lambda_4+10\lambda_5\right)+\lambda_7\left(3\lambda_3+2\lambda_4+2\lambda_5\right)\right]\Theta_Z-\lambda_6\left(3\gamma_1^{(1)}+\gamma_2^{(1)}\right), \tag{A.18}$$

$$\beta^{(1)}_{\lambda_7} = -2\left[\lambda_7\left(12\lambda_2+3\lambda_3+4\lambda_4+10\lambda_5\right)+\lambda_6\left(3\lambda_3+2\lambda_4+2\lambda_5\right)\right]\Theta_Z-\lambda_7\left(\gamma_1^{(1)}+3\gamma_2^{(1)}\right), \tag{A.19}$$

$$\gamma_1^{(1)} = \frac{1}{4}\left[\left(9g^2+3g'^2-4\left(N_Ch_b^2+h_\tau^2\right)\right)\Theta_Z-6g^2\Theta_{\widetilde{W}}\Theta_{\widetilde{H}}-2g'^2\Theta_{\widetilde{B}}\Theta_{\widetilde{H}}\right], \tag{A.20}$$

$$\gamma_2^{(1)} = \frac{1}{4}\left[\left(9g^2+3g'^2-4N_Ch_t^2\Theta_t\right)\Theta_Z-6g^2\Theta_{\widetilde{W}}\Theta_{\widetilde{H}}-2g'^2\Theta_{\widetilde{B}}\Theta_{\widetilde{H}}\right], \tag{A.21}$$

$$\beta^{(1)}_{h_t} = \left(\frac{9}{2}h_t^2+\frac{1}{2}h_b^2-8g_s^2-\frac{9}{4}g^2-\frac{17}{12}g'^2\right)h_t, \tag{A.22}$$

$$\beta^{(1)}_{h_b} = \left(\frac{9}{2}h_b^2+\frac{1}{2}h_t^2+h_\tau^2-8g_s^2-\frac{9}{4}g^2-\frac{5}{12}g'^2\right)h_b, \tag{A.23}$$

$$\beta^{(1)}_{h_\tau} = \left(\frac{5}{2}h_\tau^2+3h_b^2-\frac{9}{4}g^2-\frac{15}{4}g'^2\right)h_\tau, \tag{A.24}$$

$$\beta^{(1)}_{g'} = \left\{\frac{1}{4}N_C\sum_{i=1}^{3}\left[2Y_Q^2\left(2\Theta_t+\Theta_{\widetilde{Q}_i}\right)+Y_U^2\left(2\Theta_t+\Theta_{\widetilde{U}_i}\right)+Y_D^2\left(2\Theta_t+\Theta_{\widetilde{D}_i}\right)\right]\right.$$
$$\left.+\frac{1}{4}\sum_{i=1}^{3}\left[2Y_L^2\left(2\Theta_t+\Theta_{\widetilde{L}_i}\right)+Y_E^2\left(2\Theta_t+\Theta_{\widetilde{E}_i}\right)\right]+\frac{1}{2}N_H\Theta_t+N_{\widetilde{H}}\Theta_{\widetilde{H}}\right\}\frac{g'^3}{3}, \tag{A.25}$$

with $N_H = 2$ and $N_{\widetilde{H}} = 2$,

$$\beta^{(1)}_g = \left\{\frac{1}{2}N_C\sum_{i=1}^{3}\left(2\Theta_t+\Theta_{\widetilde{Q}_i}\right)+\frac{1}{2}\sum_{i=1}^{3}\left(2\Theta_t+\Theta_{\widetilde{L}_i}\right)+\frac{1}{2}N_H\Theta_t+N_{\widetilde{H}}\Theta_{\widetilde{H}}+4N_{\widetilde{W}}\Theta_{\widetilde{W}}-22\Theta_t\right\}\frac{g^3}{3}, \tag{A.26}$$

with $N_{\widetilde{W}} = 1$,

$$\beta^{(1)}_{g_s} = \left\{2N_f+\sum_{i=1}^{3}\left(\Theta_{\widetilde{Q}_i}+\frac{1}{2}\Theta_{\widetilde{U}_i}+\frac{1}{2}\Theta_{\widetilde{D}_i}\right)+6N_{\tilde{g}}\Theta_{\tilde{g}}-33\right\}\frac{g_s^3}{3}, \tag{A.27}$$

JHEP02(2016)123

with $N_f = \Theta_t + \Theta_b + \Theta_c + \Theta_s + \Theta_d + \Theta_u$ and $N_{\tilde{g}} = 1$,

$$\begin{aligned}\beta^{(1)}_{\tan\beta} &= \left(\gamma_2^{(1)} - \gamma_1^{(1)}\right)\tan\beta \\ &= \left(-N_C h_t^2 \Theta_t \Theta_Z + N_C h_b^2 \Theta_Z + h_\tau^2 \Theta_Z\right)\tan\beta\,, \end{aligned} \tag{A.28}$$

$$\beta^{(1)}_{\mu_1^2} = -2\left[6\mu_1^2\lambda_1 + \mu_2^2(2\lambda_3+\lambda_4) + 6m_{12}^2\lambda_6\right] - 2\gamma_1^{(1)}\mu_1^2\,, \tag{A.29}$$

$$\beta^{(1)}_{\mu_2^2} = -2\left[6\mu_2^2\lambda_2 + \mu_1^2(2\lambda_3+\lambda_4) + 6m_{12}^2\lambda_7\right] - 2\gamma_2^{(1)}\mu_2^2\,, \tag{A.30}$$

$$\beta^{(1)}_{m_{12}^2} = 2\left[-(\lambda_3+2\lambda_4+6\lambda_5)m_{12}^2 - 3\lambda_6\mu_1^2 - 3\lambda_7\mu_2^2\right] - \left(\gamma_1^{(1)} + \gamma_2^{(1)}\right)m_{12}^2\,. \tag{A.31}$$

A.3 Two-loop 2HDM RGEs

In this appendix, we present the RGEs of the general 2HDM at the two-loop order, as derived in [32, 33]. For definiteness, we follow the conventions of [33], where $g_3 \to g_s$, $g_2 \to g$, $g_1^2 \to (5/3)g'^2$; $\lambda_{1,2,5} \to -2\lambda_{1,2,5}$, $\lambda_{3,4,6,7} \to -\lambda_{3,4,6,7}$. The two-loop beta functions for the quartic couplings are given by

$$\begin{aligned}\beta^{(2)}_{\lambda_1} =& -\frac{291}{16}g^6 + \frac{101}{16}g^4g'^2 + \frac{191}{16}g^2g'^4 + \frac{131}{16}g'^6 \\ &+\frac{3}{16}g^4\left[12h_b^2 + 4h_\tau^2 - 34\lambda_1 + 20(2\lambda_3+\lambda_4)\right] - \frac{1}{8}g^2g'^2\left[36h_b^2 + 44h_\tau^2 - 78\lambda_1 - 20\lambda_4\right] \\ &-\frac{1}{16}g'^4\left[20h_b^2 - 100h_\tau^2 - 434\lambda_1 - 20(2\lambda_3+\lambda_4)\right] \\ &+8g_s^2h_b^2\left[4h_b^2+10\lambda_1\right] - \frac{3}{4}g^2\left[-10\lambda_1\left(3h_b^2+h_\tau^2\right) + 4\left(36\lambda_1^2+4\lambda_3^2+4\lambda_3\lambda_4+\lambda_4^2+18\lambda_6^2\right)\right] \\ &-\frac{1}{12}g'^2\left[h_b^2\left(16h_b^2 - 50\lambda_1\right) + 3h_\tau^2\left(-16h_\tau^2 - 50\lambda_1\right)\right. \\ &\left.+12\left(36\lambda_1^2 + 4\lambda_3^2 + 4\lambda_3\lambda_4 + 2\lambda_4^2 - 4\lambda_5^2 + 18\lambda_6^2\right)\right] \\ &+6h_t^2\left[2\lambda_3^2 + 2\lambda_3\lambda_4 + \lambda_4^2 + 4\lambda_5^2 + 6\lambda_6^2\right] - \frac{3}{2}h_t^2h_b^2\left[4h_b^2 + 6\lambda_1\right] \\ &+\frac{3}{2}h_b^2\left[-20h_b^4 - 2h_b^2\lambda_1 + 96\lambda_1^2 + 24\lambda_6^2\right] + \frac{1}{2}h_\tau^2\left[-20h_\tau^4 - 2h_\tau^2\lambda_1 + 96\lambda_1^2 + 24\lambda_6^2\right] \\ &-2\lambda_1\left[156\lambda_1^2 + 10\lambda_3^2 + 10\lambda_3\lambda_4 + 6\lambda_4^2 + 28\lambda_5^2 + 159\lambda_6^2 - 3\lambda_7^2\right] \\ &-2\lambda_3\left[4\lambda_3^2 + 6\lambda_3\lambda_4 + 8\lambda_4^2 + 40\lambda_5^2 + 33\lambda_6^2 + 18\lambda_6\lambda_7 + 9\lambda_7^2\right] \\ &-2\lambda_4\left[3\lambda_4^2 + 44\lambda_5^2 + 35\lambda_6^2 + 14\lambda_6\lambda_7 + 7\lambda_7^2\right] - 4\lambda_5\left[37\lambda_6^2 + 10\lambda_6\lambda_7 + 5\lambda_7^2\right]\,, \end{aligned} \tag{A.32}$$

$$\begin{aligned}\beta^{(2)}_{\lambda_2} =& -\frac{291}{16}g^6 + \frac{101}{16}g^4g'^2 + \frac{191}{16}g^2g'^4 + \frac{131}{16}g'^6 \\ &+\frac{3}{16}g^4\left[12h_t^2 - 34\lambda_2 + 20(2\lambda_3+\lambda_4)\right] - \frac{1}{8}g^2g'^2\left[84h_t^2 - 78\lambda_2 - 20\lambda_4\right] \\ &+\frac{1}{16}g'^4\left[76h_t^2 + 434\lambda_2 + 20(2\lambda_3+\lambda_4)\right] \\ &+8g_s^2h_t^2\left[4h_t^2 + 10\lambda_2\right] - \frac{3}{4}g^2\left[-30h_t^2\lambda_2 + 4\left(36\lambda_2^2 + 4\lambda_3^2 + 4\lambda_3\lambda_4 + \lambda_4^2 + 18\lambda_7^2\right)\right] \\ &-\frac{1}{12}g'^2\left[-h_t^2\left(32h_t^2 + 170\lambda_2\right) + 12\left(36\lambda_2^2 + 4\lambda_3^2 + 4\lambda_3\lambda_4 + 2\lambda_4^2 - 4\lambda_5^2 + 18\lambda_7^2\right)\right] \\ &-\frac{3}{2}h_t^2\left[20h_t^4 + 2h_t^2\lambda_2 - 96\lambda_2^2 - 24\lambda_7^2\right] - \frac{3}{2}h_t^2h_b^2\left[4h_t^2 + 6\lambda_2\right] \end{aligned}$$

JHEP02(2016)123

$$
\begin{aligned}
&+(6h_b^2+2h_\tau^2)\left[2\lambda_3^2+2\lambda_3\lambda_4+\lambda_4^2+4\lambda_5^2+6\lambda_7^2\right]\\
&-2\lambda_2\left[156\lambda_2^2+10\lambda_3^2+10\lambda_3\lambda_4+6\lambda_4^2+28\lambda_5^2-3\lambda_6^2+159\lambda_7^2\right]\\
&-2\lambda_3\left[4\lambda_3^2+6\lambda_3\lambda_4+8\lambda_4^2+40\lambda_5^2+9\lambda_6^2+18\lambda_6\lambda_7+33\lambda_7^2\right]\\
&-2\lambda_4\left[3\lambda_4^2+44\lambda_5^2+7\lambda_6^2+14\lambda_6\lambda_7+35\lambda_7^2\right]-4\lambda_5\left[5\lambda_6^2+10\lambda_6\lambda_7+37\lambda_7^2\right]\ , \qquad \text{(A.33)}\\
\beta^{(2)}_{\lambda_3} =\ &-\frac{291}{8}g^6-\frac{11}{8}g^4g'^2-\frac{101}{8}g^2g'^4+\frac{131}{8}g'^6\\
&+\frac{3}{4}g^4\left[3h_t^2+3h_b^2+h_\tau^2+30(\lambda_1+\lambda_2)-\frac{37}{2}\lambda_3+10\lambda_4\right]\\
&+\frac{1}{2}g^2g'^2\left[21h_t^2+9h_b^2+11h_\tau^2-10(\lambda_1+\lambda_2)+\frac{11}{2}\lambda_3-6\lambda_4\right]\\
&-\frac{1}{8}g'^4\left[-38h_t^2+10h_b^2-50h_\tau^2-60(\lambda_1+\lambda_2)-197\lambda_3-20\lambda_4\right]\\
&+8g_s^2\left[8h_t^2h_b^2+5\lambda_3\left(h_t^2+h_b^2\right)\right]\\
&-6g^2\left[-\frac{5}{8}\lambda_3\left(3h_t^2+3h_b^2+h_\tau^2\right)+6(\lambda_1+\lambda_2)(2\lambda_3+\lambda_4)+(\lambda_3-\lambda_4)^2+18\lambda_6\lambda_7\right]\\
&-\frac{1}{3}g'^2\left[-4h_t^2h_b^2-\frac{5}{4}\lambda_3\left(17h_t^2+5h_b^2+15h_\tau^2\right)\right.\\
&\left.+24(\lambda_1+\lambda_2)(3\lambda_3+\lambda_4)+6\left(\lambda_3^2-\lambda_4^2+8\lambda_5^2+\lambda_6^2+16\lambda_6\lambda_7+\lambda_7^2\right)\right]\\
&+\frac{9}{2}\lambda_3\left[3h_t^4+3h_b^4+h_\tau^4\right]-h_t^2h_b^2\left[36\left(h_t^2+h_b^2\right)-15\lambda_3\right]\\
&+6h_t^2\left[12\lambda_2\lambda_3+4\lambda_2\lambda_4+2\lambda_3^2+\lambda_4^2+4\lambda_5^2+8\lambda_6\lambda_7+4\lambda_7^2\right]\\
&+\left(6h_b^2+2h_\tau^2\right)\left[12\lambda_1\lambda_3+4\lambda_1\lambda_4+2\lambda_3^2+\lambda_4^2+4\lambda_5^2+4\lambda_6^2+8\lambda_6\lambda_7\right]\\
&-4\left(\lambda_1^2+\lambda_2^2\right)\left[15\lambda_3+4\lambda_4\right]-4(\lambda_1+\lambda_2)\left[18\lambda_3^2+8\lambda_3\lambda_4+7\lambda_4^2+36\lambda_5^2\right]\\
&-4\lambda_1\left[31\lambda_6^2+22\lambda_6\lambda_7+11\lambda_7^2\right]-4\lambda_2\left[11\lambda_6^2+22\lambda_6\lambda_7+31\lambda_7^2\right]\\
&-\lambda_3\left[12\lambda_3^2+4\lambda_3\lambda_4+16\lambda_4^2+72\lambda_5^2+60\lambda_6^2+176\lambda_6\lambda_7+60\lambda_7^2\right]\\
&-\lambda_4\left[12\lambda_4^2+176\lambda_5^2+68\lambda_6^2+88\lambda_6\lambda_7+68\lambda_7^2\right]\\
&-2\lambda_5\left[68\lambda_6^2+72\lambda_6\lambda_7+68\lambda_7^2\right]\ , \qquad \text{(A.34)}\\
\beta^{(2)}_{\lambda_4} =\ &+14g^4g'^2+\frac{73}{2}g^2g'^4+\lambda_4\left[-\frac{231}{8}g^4+\frac{157}{8}g'^4\right]\\
&-\frac{1}{2}g^2g'^2\left[42h_t^2+18h_b^2+22h_\tau^2-20\lambda_1-20\lambda_2-4\lambda_3-\frac{51}{2}\lambda_4\right]\\
&-8g_s^2\left[8h_t^2h_b^2-5\lambda_4\left(h_t^2+h_b^2\right)\right]\\
&-g^2\left[-\frac{15}{4}\lambda_4\left(3h_t^2+3h_b^2+h_\tau^2\right)+18\left(2\lambda_3\lambda_4+\lambda_4^2+12\lambda_5^2+3\lambda_6^2+3\lambda_7^2\right)\right]\\
&-\frac{1}{3}g'^2\left[4h_t^2h_b^2-\frac{5}{4}\lambda_4\left(17h_t^2+5h_b^2+15h_\tau^2\right)+12\lambda_4(2\lambda_1+2\lambda_2+\lambda_3+2\lambda_4)\right.\\
&\left.+6\left(32\lambda_5^2+7\lambda_6^2+4\lambda_6\lambda_7+7\lambda_7^2\right)\right]\\
&-\frac{9}{2}\lambda_4\left[3h_t^4+3h_b^4+h_\tau^4\right]+h_t^2h_b^2\left[24\left(h_t^2+h_b^2\right)-24\lambda_3-33\lambda_4\right]\\
&+12h_t^2\left[2\lambda_2\lambda_4+2\lambda_3\lambda_4+\lambda_4^2+8\lambda_5^2+\lambda_6\lambda_7+5\lambda_7^2\right]
\end{aligned}
$$

JHEP02(2016)123

$$
\begin{aligned}
&+\left(12h_b^2+4h_\tau^2\right)\left[2\lambda_1\lambda_4+2\lambda_3\lambda_4+\lambda_4^2+8\lambda_5^2+5\lambda_6^2+\lambda_6\lambda_7\right]\\
&-28\lambda_4\left[\lambda_1^2+\lambda_2^2\right]-8(\lambda_1+\lambda_2)\left[10\lambda_3\lambda_4+5\lambda_4^2+24\lambda_5^2\right]\\
&-4\lambda_1\left[37\lambda_6^2+10\lambda_6\lambda_7+5\lambda_7^2\right]-4\lambda_2\left[5\lambda_6^2+10\lambda_6\lambda_7+37\lambda_7^2\right]\\
&-4\lambda_3\left[7\lambda_3\lambda_4+7\lambda_4^2+48\lambda_5^2+18\lambda_6^2+20\lambda_6\lambda_7+18\lambda_7^2\right]\\
&-2\lambda_4\left[52\lambda_5^2+34\lambda_6^2+80\lambda_6\lambda_7+34\lambda_7^2\right]-32\lambda_5\left[5\lambda_6^2+6\lambda_6\lambda_7+5\lambda_7^2\right]\ , \qquad \text{(A.35)}
\end{aligned}
$$

$$
\begin{aligned}
\beta^{(2)}_{\lambda_5} =\ &+\lambda_5\left[-\frac{231}{8}g^4+\frac{19}{4}g^2g'^2+\frac{157}{8}g'^4\right]+40g_s^2\lambda_5\left[h_t^2+h_b^2\right]\\
&-\frac{3}{8}g^2\left[-10\lambda_5\left(3h_t^2+3h_b^2+h_\tau^2\right)+96\lambda_5(\lambda_3+2\lambda_4)+72\left(\lambda_6^2+\lambda_7^2\right)\right]\\
&-\frac{1}{24}g'^2\left[-10\lambda_5\left(17h_t^2+5h_b^2+15h_\tau^2\right)-48\lambda_5(2\lambda_1+2\lambda_2-8\lambda_3-12\lambda_4)\right.\\
&\left.+48\left(5\lambda_6^2-\lambda_6\lambda_7+5\lambda_7^2\right)\right]\\
&-\frac{1}{2}\lambda_5\left[3h_t^4+3h_b^4+h_\tau^4\right]-h_t^2\left[33h_b^2\lambda_5-12\lambda_5(2\lambda_2+2\lambda_3+3\lambda_4)-6\lambda_7(\lambda_6+5\lambda_7)\right]\\
&+\left(6h_b^2+2h_\tau^2\right)\left[2\lambda_5(2\lambda_1+2\lambda_3+3\lambda_4)+\lambda_6(5\lambda_6+\lambda_7)\right]\\
&-28\lambda_5\left[\lambda_1^2+\lambda_2^2\right]-8\lambda_5(\lambda_1+\lambda_2)(10\lambda_3+11\lambda_4)\\
&-2\lambda_1\left[37\lambda_6^2+10\lambda_6\lambda_7+5\lambda_7^2\right]-2\lambda_2\left[5\lambda_6^2+10\lambda_6\lambda_7+37\lambda_7^2\right]\\
&-2\lambda_3\left[14\lambda_3\lambda_5+38\lambda_4\lambda_5+18\lambda_6^2+20\lambda_6\lambda_7+18\lambda_7^2\right]\\
&-2\lambda_4\left[16\lambda_4\lambda_5+19\lambda_6^2+22\lambda_6\lambda_7+19\lambda_7^2\right]+24\lambda_5^3-8\lambda_5\left[9\lambda_6^2+21\lambda_6\lambda_7+9\lambda_7^2\right]\ , \qquad \text{(A.36)}
\end{aligned}
$$

$$
\begin{aligned}
\beta^{(2)}_{\lambda_6} =\ &+\frac{1}{8}g^4[-141\lambda_6+90\lambda_7]+\frac{1}{4}g^2g'^2[29\lambda_6+10\lambda_7]+\frac{1}{8}g'^4[187\lambda_6+30\lambda_7]+20g_s^2\lambda_6\left[h_t^2+3h_b^2\right]\\
&+\frac{9}{8}g^2\left[5\lambda_6\left(h_t^2+3h_b^2+h_\tau^2\right)-96\lambda_6(\lambda_1+\lambda_5)-16\lambda_6(\lambda_3+2\lambda_4)-16\lambda_7(2\lambda_3+\lambda_4)\right]\\
&+\frac{1}{24}g'^2\left[5\lambda_6\left(17h_t^2+15h_b^2+45h_\tau^2\right)-48\lambda_6(18\lambda_1+3\lambda_3+5\lambda_4+20\lambda_5)\right.\\
&\left.-48\lambda_7(6\lambda_3+4\lambda_4-2\lambda_5)\right]\\
&-\frac{1}{4}\lambda_6\left[27h_t^4+84h_t^2h_b^2+33h_b^4+11h_\tau^4\right]\\
&+6h_t^2\left[\lambda_6(3\lambda_3+4\lambda_4+10\lambda_5)+\lambda_7(6\lambda_3+4\lambda_4+4\lambda_5)\right]\\
&+\left(6h_b^2+2h_\tau^2\right)\lambda_6\left[24\lambda_1+3\lambda_3+4\lambda_4+10\lambda_5\right]\\
&-6\lambda_6\left[53\lambda_1^2-\lambda_2^2\right]-4\lambda_1\lambda_6\left[33\lambda_3+35\lambda_4+74\lambda_5\right]-4\lambda_2\lambda_6\left[9\lambda_3+7\lambda_4+10\lambda_5\right]\\
&-2\lambda_6\left[16\lambda_3^2+34\lambda_3\lambda_4+72\lambda_3\lambda_5+17\lambda_4^2+76\lambda_4\lambda_5+72\lambda_5^2\right]\\
&-4(\lambda_1+\lambda_2)\lambda_7\left[9\lambda_3+7\lambda_4+10\lambda_5\right]\\
&-2\lambda_7\left[18\lambda_3^2+28\lambda_3\lambda_4+40\lambda_3\lambda_5+17\lambda_4^2+44\lambda_4\lambda_5+84\lambda_5^2\right]\\
&-3\left[37\lambda_6^3+42\lambda_6^2\lambda_7+11\lambda_6\lambda_7^2+14\lambda_7^3\right]\ , \qquad \text{(A.37)}
\end{aligned}
$$

$$
\begin{aligned}
\beta^{(2)}_{\lambda_7} =\ &+\frac{1}{8}g^4\left[90\lambda_6-141\lambda_7\right]+\frac{1}{4}g^2g'^2\left[10\lambda_6+29\lambda_7\right]+\frac{1}{8}g'^4\left[30\lambda_6+187\lambda_7\right]+20g_s^2\lambda_6\left[3h_t^2+h_b^2\right]\\
&+\frac{3}{8}g^2\left[5\lambda_7\left(9h_t^2+3h_b^2+h_\tau^2\right)-288\lambda_7(\lambda_2+\lambda_5)-48\lambda_3(2\lambda_6+\lambda_7)-48\lambda_4(\lambda_6+2\lambda_7)\right]\\
&+\frac{1}{24}g'^2\left[5\lambda_7\left(51h_t^2+5h_b^2+15h_\tau^2\right)-48\lambda_6(6\lambda_3+4\lambda_4-2\lambda_5)\right.
\end{aligned}
$$

JHEP02(2016)123

$$
\begin{aligned}
&-48\lambda_7(18\lambda_2+3\lambda_3+5\lambda_4+20\lambda_5)]\\
&-\frac{3}{4}\lambda_7\left[11h_t^4+28h_t^2h_b^2+9h_b^4+3h_\tau^4\right]\\
&+6h_t^2\lambda_7\left[24\lambda_2+3\lambda_3+4\lambda_4+10\lambda_5\right]\\
&+(6h_b^2+2h_\tau^2)\left[\lambda_6(6\lambda_3+4\lambda_4+4\lambda_5)+\lambda_7(3\lambda_3+4\lambda_4+10\lambda_5)\right]\\
&-6\lambda_7\left[-\lambda_1^2+53\lambda_2^2\right]-4\lambda_1\lambda_7\left[9\lambda_3+7\lambda_4+10\lambda_5\right]-4\lambda_2\lambda_7\left[33\lambda_3+35\lambda_4+74\lambda_5\right]\\
&-2\lambda_7\left[16\lambda_3^2+34\lambda_3\lambda_4+72\lambda_3\lambda_5+17\lambda_4^2+76\lambda_4\lambda_5+72\lambda_5^2\right]\\
&-4(\lambda_1+\lambda_2)\lambda_6\left[9\lambda_3+7\lambda_4+10\lambda_5\right]\\
&-2\lambda_6\left[18\lambda_3^2+28\lambda_3\lambda_4+40\lambda_3\lambda_5+17\lambda_4^2+44\lambda_4\lambda_5+84\lambda_5^2\right]\\
&-3\left[14\lambda_6^3+11\lambda_6^2\lambda_7+42\lambda_6\lambda_7^2+37\lambda_7^3\right]\ . \qquad \text{(A.38)}
\end{aligned}
$$

In addition, the two-loop beta functions for the gauge and the supersymmetric Yukawa couplings may be listed as follows:

$$\beta_{g'}^{(2)}=\frac{5}{3}g'^3\left(\frac{44}{5}g_s^2+\frac{18}{5}g^2+\frac{104}{15}g'^2-\frac{17}{10}h_t^2-\frac{1}{2}h_b^2-\frac{3}{2}h_\tau^2\right), \qquad \text{(A.39)}$$

$$\beta_{g}^{(2)}=g^3\left(12g_s^2+8g^2+2g'^2-\frac{3}{2}h_t^2-\frac{3}{2}h_b^2-\frac{1}{2}h_\tau^2\right), \qquad \text{(A.40)}$$

$$\beta_{g_s}^{(2)}=g_s^3\left(-26g_s^2+\frac{9}{2}g^2+\frac{11}{6}g'^2-2h_t^2-2h_b^2\right), \qquad \text{(A.41)}$$

$$
\begin{aligned}
\beta_{h_t}^{(2)}=h_t\Bigg[&-108g_s^4+9g_s^2g^2+\frac{19}{9}g_s^2g'^2-\frac{21}{4}g^4-\frac{3}{4}g^2g'^2+\frac{1267}{216}g'^4\\
&+g_s^2\left(36h_t^2+\frac{16}{3}h_b^2\right)+\frac{3}{16}g^2\left(75h_t^2+11h_b^2\right)+\frac{1}{48}g'^2\left(393h_t^2-\frac{41}{3}h_b^2\right)\\
&-12h_t^4-\frac{5}{2}h_t^2h_b^2-\frac{5}{2}h_b^4-\frac{3}{4}h_b^2h_\tau^2+12h_t^2\lambda_2+2h_b^2(\lambda_3-\lambda_4)\\
&+6\lambda_2^2+\lambda_3^2+\lambda_3\lambda_4+\lambda_4^2+6\lambda_5^2+\frac{3}{2}\lambda_6^2+\frac{9}{2}\lambda_7^2\Bigg], \qquad \text{(A.42)}
\end{aligned}
$$

$$
\begin{aligned}
\beta_{h_b}^{(2)}=h_b\Bigg[&-108g_s^4+9g_s^2g^2+\frac{31}{9}g_s^2g'^2-\frac{21}{4}g^4-\frac{9}{4}g^2g'^2+\frac{113}{216}g'^4\\
&+g_s^2\left(\frac{16}{3}h_t^2+36h_b^2\right)+\frac{3}{16}g^2\left(11h_t^2+75h_b^2+10h_\tau^2\right)-\frac{1}{144}g'^2\left(53h_t^2-711h_b^2-450h_\tau^2\right)\\
&-\frac{5}{2}h_t^4-\frac{5}{2}h_t^2h_b^2-12h_b^4-\frac{9}{4}h_b^2h_\tau^2-\frac{9}{4}h_\tau^4+12h_b^2\lambda_1+2h_t^2(\lambda_3-\lambda_4)\\
&+6\lambda_1^2+\lambda_3^2+\lambda_3\lambda_4+\lambda_4^2+6\lambda_5^2+\frac{9}{2}\lambda_6^2+\frac{3}{2}\lambda_7^2\Bigg], \qquad \text{(A.43)}
\end{aligned}
$$

$$
\begin{aligned}
\beta_{h_\tau}^{(2)}=h_\tau\Bigg[&20g_s^2h_b^2-\frac{21}{4}g^4+\frac{9}{4}g^2g'^2+\frac{161}{8}g'^4\\
&+\frac{15}{16}g^2\left(6h_b^2+11h_\tau^2\right)+\frac{1}{48}g'^2\left(50h_b^2+537h_\tau^2\right)
\end{aligned}
$$

JHEP02(2016)123

$$
\begin{aligned}
&-\frac{9}{4}h_t^2h_b^2-\frac{27}{4}h_b^4-\frac{27}{4}h_b^2h_\tau^2-3h_\tau^4+12h_\tau^2\lambda_1\\
&+6\lambda_1^2+\lambda_3^2+\lambda_3\lambda_4+\lambda_4^2+6\lambda_5^2+\frac{9}{2}\lambda_6^2+\frac{3}{2}\lambda_7^2\Bigg]\,. \qquad \text{(A.44)}
\end{aligned}
$$

Finally, the two-loop anomalous dimensions for the Higgs doublets are given by

$$
\begin{aligned}
\gamma_1^{(2)} &= \frac{435}{32}g^4-\frac{3}{16}g^2g'^2-\frac{149}{32}g'^4-20g_s^2h_b^2-\frac{15}{8}g^2\left(3h_b^2+h_\tau^2\right)-\frac{25}{24}g'^2\left(h_b^2+3h_\tau^2\right)\\
&\quad+\frac{9}{4}h_t^2h_b^2+\frac{27}{4}h_b^4+\frac{9}{4}h_\tau^4-6\lambda_1^2-\lambda_3^2-\lambda_3\lambda_4-\lambda_4^2-6\lambda_5^2-\frac{9}{2}\lambda_6^2-\frac{3}{2}\lambda_7^2\\
&\quad-\frac{3}{2}t_\beta\left[2\lambda_1\lambda_6+2\lambda_2\lambda_7+(\lambda_3+\lambda_4+2\lambda_5)(\lambda_6+\lambda_7)\right]\,, \qquad \text{(A.45)}\\
\gamma_2^{(2)} &= \frac{435}{32}g^4-\frac{3}{16}g^2g'^2-\frac{149}{32}g'^4-h_t^2\left(20g_s^2+\frac{45}{8}g^2+\frac{85}{24}g'^2\right)\\
&\quad+\frac{27}{4}h_t^4+\frac{9}{4}h_b^2h_t^2-6\lambda_2^2-\lambda_3^2-\lambda_3\lambda_4-\lambda_4^2-6\lambda_5^2-\frac{3}{2}\lambda_6^2-\frac{9}{2}\lambda_7^2\\
&\quad-\frac{3}{2}t_\beta^{-1}\left[2\lambda_1\lambda_6+2\lambda_2\lambda_7+(\lambda_3+\lambda_4+2\lambda_5)(\lambda_6+\lambda_7)\right]\,. \qquad \text{(A.46)}
\end{aligned}
$$

A.4 Threshold corrections to λ_i at M_S

At the soft SUSY-breaking scale $Q=M_S$, we need to consider the threshold corrections to quartic couplings due to third-generation sfermions. These are derived in [33], which we extend here to include CP-violating phases.

The quartic couplings λ_i with $i=1-7$ at the RG scale $Q=M_S$ are given by

$$
\lambda_i(M_S)=\lambda_i^{(0)}+\sum_{n=1,2}\kappa^n\Delta^{(n)}\lambda_i\,, \qquad \text{(A.47)}
$$

where

$$
\begin{aligned}
&\lambda_1^{(0)}=\lambda_2^{(0)}=-\frac{1}{8}\left(g^2+g'^2\right)\,,\quad \lambda_3^{(0)}=-\frac{1}{4}\left(g^2-g'^2\right)\,,\quad \lambda_4^{(0)}=\frac{1}{2}\,g^2\,,\\
&\lambda_5^{(0)}=\lambda_6^{(0)}=\lambda_7^{(0)}=0\,, \qquad \text{(A.48)}
\end{aligned}
$$

and the one- and two-loop threshold corrections are[6]

$$
\begin{aligned}
\Delta^{(1)}\lambda_1 &= \frac{1}{4}|h_t|^4|\widehat{\mu}|^4-3|h_b|^4|\widehat{A}_b|^2\left(1-\frac{|\widehat{A}_b|^2}{12}\right)-|h_\tau|^4|\widehat{A}_\tau|^2\left(1-\frac{|\widehat{A}_\tau|^2}{12}\right)\\
&\quad-\frac{g^2+g'^2}{8}\left(3|h_t|^2|\widehat{\mu}|^2-3|h_b|^2|\widehat{A}_b|^2-|h_\tau|^2|\widehat{A}_\tau|^2\right)\\
&\quad+\frac{g^2+g'^2}{24}\left(3|h_t|^2|\widehat{\mu}|^2+3|h_b|^2|\widehat{A}_b|^2+|h_\tau|^2|\widehat{A}_\tau|^2\right)\,, \qquad \text{(A.49)}\\
\Delta^{(1)}\lambda_2 &= -3|h_t|^4|\widehat{A}_t|^2\left(1-\frac{|\widehat{A}_t|^2}{12}\right)+\frac{1}{4}|h_b|^4|\widehat{\mu}|^4+\frac{1}{12}|h_\tau|^4|\widehat{\mu}|^4
\end{aligned}
$$

[6]Here all the mass parameters are dimensionsless and normalized to the SUSY scale M_S: $\widehat{\mu}=\mu/M_S$, $\widehat{A}_{t,b,\tau}=A_{t,b,\tau}/M_S$, and $\widehat{M}_3=M_3/M_S$.

JHEP02(2016)123

$$
\begin{aligned}
&+\frac{g^2+g'^2}{8}\left(3|h_t|^2|\widehat{A}_t|^2-3|h_b|^2|\widehat{\mu}|^2-|h_\tau|^2|\widehat{\mu}|^2\right)\\
&+\frac{g^2+g'^2}{24}\left(3|h_t|^2|\widehat{A}_t|^2+3|h_b|^2|\widehat{\mu}|^2+|h_\tau|^2|\widehat{\mu}|^2\right), \qquad \text{(A.50)}
\end{aligned}
$$

$$
\begin{aligned}
\Delta^{(1)}\lambda_3 =\ & -\frac{1}{6}|\mu|^2\left[3|h_t|^4\left(3-|\widehat{A}_t|^2\right)+3|h_b|^4\left(3-|\widehat{A}_b|^2\right)+|h_\tau|^4\left(3-|\widehat{A}_\tau|^2\right)\right]\\
&-\frac{1}{2}|h_t|^2|h_b|^2\left[3|\widehat{A}_t+\widehat{A}_b|^2-||\widehat{\mu}|^2-\widehat{A}_t\widehat{A}_b^*|^2-6|\widehat{\mu}|^2\right]\\
&+\frac{g^2-g'^2}{8}\left[3|h_t|^2\left(|\widehat{A}_t|^2-|\widehat{\mu}|^2\right)+3|h_b|^2\left(|\widehat{A}_b|^2-|\widehat{\mu}|^2\right)+|h_\tau|^2\left(|\widehat{A}_\tau|^2-|\widehat{\mu}|^2\right)\right]\\
&+\frac{g^2-g'^2}{24}\left[3|h_t|^2\left(|\widehat{A}_t|^2+|\widehat{\mu}|^2\right)+3|h_b|^2\left(|\widehat{A}_b|^2+|\widehat{\mu}|^2\right)+|h_\tau|^2\left(|\widehat{A}_\tau|^2+|\widehat{\mu}|^2\right)\right], \qquad \text{(A.51)}
\end{aligned}
$$

$$
\begin{aligned}
\Delta^{(1)}\lambda_4 =\ & -\frac{1}{6}|\mu|^2\left[3|h_t|^4\left(3-|\widehat{A}_t|^2\right)+3|h_b|^4\left(3-|\widehat{A}_b|^2\right)+|h_\tau|^4\left(3-|\widehat{A}_\tau|^2\right)\right]\\
&+\frac{1}{2}|h_t|^2|h_b|^2\left[3|\widehat{A}_t+\widehat{A}_b|^2-||\widehat{\mu}|^2-\widehat{A}_t\widehat{A}_b^*|^2-6|\widehat{\mu}|^2\right]\\
&-\frac{g^2}{4}\left[3|h_t|^2\left(|\widehat{A}_t|^2-|\widehat{\mu}|^2\right)+3|h_b|^2\left(|\widehat{A}_b|^2-|\widehat{\mu}|^2\right)+|h_\tau|^2\left(|\widehat{A}_\tau|^2-|\widehat{\mu}|^2\right)\right]\\
&-\frac{g^2}{12}\left[3|h_t|^2\left(|\widehat{A}_t|^2+|\widehat{\mu}|^2\right)+3|h_b|^2\left(|\widehat{A}_b|^2+|\widehat{\mu}|^2\right)+|h_\tau|^2\left(|\widehat{A}_\tau|^2+|\widehat{\mu}|^2\right)\right], \qquad \text{(A.52)}
\end{aligned}
$$

$$
\Delta^{(1)}\lambda_5 = \frac{1}{12}\left[3h_t^4\widehat{\mu}^2\widehat{A}_t^2+3h_b^4\widehat{\mu}^2\widehat{A}_b^2+h_\tau^4\widehat{\mu}^2\widehat{A}_\tau^2\right], \qquad \text{(A.53)}
$$

$$
\Delta^{(1)}\lambda_6 = -\frac{1}{6}\left[3h_t^4|\widehat{\mu}|^2\widehat{\mu}\widehat{A}_t+3h_b^4\widehat{\mu}\widehat{A}_b\left(|\widehat{A}_b|^2-6\right)+h_\tau^4\widehat{\mu}\widehat{A}_\tau\left(|\widehat{A}_\tau|^2-6\right)\right], \qquad \text{(A.54)}
$$

$$
\Delta^{(1)}\lambda_7 = -\frac{1}{6}\left[3h_t^4\widehat{\mu}\widehat{A}_t\left(|\widehat{A}_t|^2-6\right)+3h_b^4|\widehat{\mu}|^2\widehat{\mu}\widehat{A}_b+h_\tau^4|\widehat{\mu}|^2\widehat{\mu}\widehat{A}_\tau\right], \qquad \text{(A.55)}
$$

where $h_{t,b,\tau}=h_{t,b,\tau}^{\rm MSSM}$ at the RG scale $Q=M_S$.

The two-loop corrections of $\mathcal{O}(|h_t|^4g_s^2)$ are given by

$$
\Delta^{(2)}\lambda_1 = \frac{2}{3}|h_t|^4g_s^2|\widehat{\mu}|^4, \qquad \text{(A.56)}
$$

$$
\Delta^{(2)}\lambda_2 = -8|h_t|^4g_s^2\left[-2\Re\mathrm{e}\left(\widehat{A}_t\widehat{M_3^*}\right)+\frac{1}{3}|\widehat{A}_t|^2\Re\mathrm{e}\left(\widehat{A}_t\widehat{M_3^*}\right)-\frac{1}{12}|\widehat{A}_t|^4\right], \qquad \text{(A.57)}
$$

$$
\Delta^{(2)}\lambda_3 = \Delta^{(2)}\lambda_4 = -\frac{8}{3}|h_t|^4g_s^2|\widehat{\mu}|^2\left[\Re\mathrm{e}\left(\widehat{A}_t\widehat{M_3^*}\right)-\frac{1}{2}|\widehat{A}_t|^2\right], \qquad \text{(A.58)}
$$

$$
\Delta^{(2)}\lambda_5 = -\frac{4}{3}|h_t|^4g_s^2\widehat{\mu}\widehat{A}_t\left[\widehat{\mu}\widehat{M_3}-\frac{1}{2}\widehat{\mu}\widehat{A}_t\right], \qquad \text{(A.59)}
$$

$$
\Delta^{(2)}\lambda_6 = -\frac{4}{3}|h_t|^4g_s^2|\widehat{\mu}|^2\left[-\widehat{\mu}\widehat{M_3}+\widehat{\mu}\widehat{A}_t\right], \qquad \text{(A.60)}
$$

$$
\Delta^{(2)}\lambda_7 = -4|h_t|^4g_s^2\left[2\widehat{\mu}\widehat{M_3}-\frac{1}{3}\widehat{\mu}\widehat{A}_t^2\widehat{M_3^*}-\frac{2}{3}|\widehat{A}_t|^2\widehat{\mu}\widehat{M_3}+\frac{1}{3}|\widehat{A}_t|^2\widehat{\mu}\widehat{A}_t\right]. \qquad \text{(A.61)}
$$

JHEP02(2016)123

References

[1] J.R. Ellis and D. Ross, *A Light Higgs boson would invite supersymmetry*, *Phys. Lett.* **B 506** (2001) 331 [hep-ph/0012067] [INSPIRE].

[2] J.R. Ellis, G. Ridolfi and F. Zwirner, *Radiative corrections to the masses of supersymmetric Higgs bosons*, *Phys. Lett.* **B 257** (1991) 83 [INSPIRE].

[3] H.E. Haber and R. Hempfling, *Can the mass of the lightest Higgs boson of the minimal supersymmetric model be larger than m(Z)?*, *Phys. Rev. Lett.* **66** (1991) 1815 [INSPIRE].

[4] Y. Okada, M. Yamaguchi and T. Yanagida, *Upper bound of the lightest Higgs boson mass in the minimal supersymmetric standard model*, *Prog. Theor. Phys.* **85** (1991) 1 [INSPIRE].

[5] ATLAS, CMS collaborations, *Combined Measurement of the Higgs Boson Mass in pp Collisions at $\sqrt{s} = 7$ and 8 TeV with the ATLAS and CMS Experiments*, *Phys. Rev. Lett.* **114** (2015) 191803 [arXiv:1503.07589] [INSPIRE].

[6] J.R. Ellis, S. Heinemeyer, K.A. Olive and G. Weiglein, *Precision analysis of the lightest MSSM Higgs boson at future colliders*, *JHEP* **01** (2003) 006 [hep-ph/0211206] [INSPIRE].

[7] ATLAS, CMS collaborations, *Measurements of the Higgs boson production and decay rates and constraints on its couplings from a combined ATLAS and CMS analysis of the LHC pp collision data at $\sqrt{s} = 7$ and 8 TeV*, ATLAS-CONF-2015-044 (2015).

[8] M. Carena, J.R. Ellis, A. Pilaftsis and C.E.M. Wagner, *CP violating MSSM Higgs bosons in the light of LEP-2*, *Phys. Lett.* **B 495** (2000) 155 [hep-ph/0009212] [INSPIRE].

[9] A. Pilaftsis, *CP odd tadpole renormalization of Higgs scalar - pseudoscalar mixing*, *Phys. Rev.* **D 58** (1998) 096010 [hep-ph/9803297] [INSPIRE].

[10] A. Pilaftsis, *Higgs scalar - pseudoscalar mixing in the minimal supersymmetric standard model*, *Phys. Lett.* **B 435** (1998) 88 [hep-ph/9805373] [INSPIRE].

[11] A. Pilaftsis and C.E.M. Wagner, *Higgs bosons in the minimal supersymmetric standard model with explicit CP-violation*, *Nucl. Phys.* **B 553** (1999) 3 [hep-ph/9902371] [INSPIRE].

[12] D.A. Demir, *Effects of the supersymmetric phases on the neutral Higgs sector*, *Phys. Rev.* **D 60** (1999) 055006 [hep-ph/9901389] [INSPIRE].

[13] S.Y. Choi, M. Drees and J.S. Lee, *Loop corrections to the neutral Higgs boson sector of the MSSM with explicit CP-violation*, *Phys. Lett.* **B 481** (2000) 57 [hep-ph/0002287] [INSPIRE].

[14] M. Carena, J.R. Ellis, A. Pilaftsis and C.E.M. Wagner, *Renormalization group improved effective potential for the MSSM Higgs sector with explicit CP-violation*, *Nucl. Phys.* **B 586** (2000) 92 [hep-ph/0003180] [INSPIRE].

[15] T. Ibrahim and P. Nath, *Corrections to the Higgs boson masses and mixings from chargino, W and charged Higgs exchange loops and large CP phases*, *Phys. Rev.* **D 63** (2001) 035009 [hep-ph/0008237] [INSPIRE].

[16] M. Carena, J.R. Ellis, A. Pilaftsis and C.E.M. Wagner, *Higgs boson pole masses in the MSSM with explicit CP-violation*, *Nucl. Phys.* **B 625** (2002) 345 [hep-ph/0111245] [INSPIRE].

JHEP02(2016)123

[17] T. Ibrahim and P. Nath, *Neutralino exchange corrections to the Higgs boson mixings with explicit CP-violation*, *Phys. Rev.* **D 66** (2002) 015005 [hep-ph/0204092] [INSPIRE].

[18] J.R. Ellis, J.S. Lee and A. Pilaftsis, *Electric Dipole Moments in the MSSM Reloaded*, *JHEP* **10** (2008) 049 [arXiv:0808.1819] [INSPIRE].

[19] T. Ibrahim and P. Nath, *The Neutron and the lepton EDMs in MSSM, large CP-violating phases and the cancellation mechanism*, *Phys. Rev.* **D 58** (1998) 111301 [*Erratum ibid.* **D 60** (1999) 099902] [hep-ph/9807501] [INSPIRE].

[20] M. Brhlik, G.J. Good and G.L. Kane, *Electric dipole moments do not require the CP-violating phases of supersymmetry to be small*, *Phys. Rev.* **D 59** (1999) 115004 [hep-ph/9810457] [INSPIRE].

[21] J. Ellis, J.S. Lee and A. Pilaftsis, *A Geometric Approach to CP-violation: applications to the MCPMFV SUSY Model*, *JHEP* **10** (2010) 049 [arXiv:1006.3087] [INSPIRE].

[22] N. Yamanaka, T. Sato and T. Kubota, *Linear programming analysis of the R-parity violation within EDM-constraints*, *JHEP* **12** (2014) 110 [arXiv:1406.3713] [INSPIRE].

[23] B. Li and C.E.M. Wagner, *CP-odd component of the lightest neutral Higgs boson in the MSSM*, *Phys. Rev.* **D 91** (2015) 095019 [arXiv:1502.02210] [INSPIRE].

[24] J.R. Ellis, J.S. Lee and A. Pilaftsis, *B-Meson Observables in the Maximally CP-Violating MSSM with Minimal Flavour Violation*, *Phys. Rev.* **D 76** (2007) 115011 [arXiv:0708.2079] [INSPIRE].

[25] A. Arbey, J. Ellis, R.M. Godbole and F. Mahmoudi, *Exploring CP-violation in the MSSM*, *Eur. Phys. J.* **C 75** (2015) 85 [arXiv:1410.4824] [INSPIRE].

[26] J.S. Lee, A. Pilaftsis, M. Carena, S.Y. Choi, M. Drees, J.R. Ellis et al., *CPsuperH: a Computational tool for Higgs phenomenology in the minimal supersymmetric standard model with explicit CP-violation*, *Comput. Phys. Commun.* **156** (2004) 283 [hep-ph/0307377] [INSPIRE].

[27] J.S. Lee, M. Carena, J. Ellis, A. Pilaftsis and C.E.M. Wagner, *CPsuperH2.0: an Improved Computational Tool for Higgs Phenomenology in the MSSM with Explicit CP-violation*, *Comput. Phys. Commun.* **180** (2009) 312 [arXiv:0712.2360] [INSPIRE].

[28] J.S. Lee, M. Carena, J. Ellis, A. Pilaftsis and C.E.M. Wagner, *CPsuperH2.3: an Updated Tool for Phenomenology in the MSSM with Explicit CP-violation*, *Comput. Phys. Commun.* **184** (2013) 1220 [arXiv:1208.2212] [INSPIRE].

[29] S. Heinemeyer, W. Hollik, H. Rzehak and G. Weiglein, *The Higgs sector of the complex MSSM at two-loop order: QCD contributions*, *Phys. Lett.* **B 652** (2007) 300 [http://www.feynhiggs.de] [arXiv:0705.0746] [INSPIRE].

[30] T. Hahn, S. Heinemeyer, W. Hollik, H. Rzehak and G. Weiglein, *High-Precision Predictions for the Light CP -Even Higgs Boson Mass of the Minimal Supersymmetric Standard Model*, *Phys. Rev. Lett.* **112** (2014) 141801 [arXiv:1312.4937] [INSPIRE].

[31] H.E. Haber and R. Hempfling, *The Renormalization group improved Higgs sector of the minimal supersymmetric model*, *Phys. Rev.* **D 48** (1993) 4280 [hep-ph/9307201] [INSPIRE].

[32] P.S. Bhupal Dev and A. Pilaftsis, *Maximally Symmetric Two Higgs Doublet Model with Natural Standard Model Alignment*, *JHEP* **12** (2014) 024 [arXiv:1408.3405] [INSPIRE].

JHEP02(2016)123

[33] G. Lee and C.E.M. Wagner, *Higgs bosons in heavy supersymmetry with an intermediate m_A*, *Phys. Rev.* **D 92** (2015) 075032 [arXiv:1508.00576] [INSPIRE].

[34] J. Guasch, W. Hollik and S. Penaranda, *Distinguishing Higgs models in $H \to b\bar{b}/H \to \tau^+\tau^-$*, *Phys. Lett.* **B 515** (2001) 367 [hep-ph/0106027] [INSPIRE].

[35] P. Draper, G. Lee and C.E.M. Wagner, *Precise estimates of the Higgs mass in heavy supersymmetry*, *Phys. Rev.* **D 89** (2014) 055023 [arXiv:1312.5743] [INSPIRE].

[36] D. Buttazzo, G. Degrassi, P.P. Giardino, G.F. Giudice, F. Sala, A. Salvio et al., *Investigating the near-criticality of the Higgs boson*, *JHEP* **12** (2013) 089 [arXiv:1307.3536] [INSPIRE].

[37] K. Melnikov and T.v. Ritbergen, *The Three loop relation between the MS-bar and the pole quark masses*, *Phys. Lett.* **B 482** (2000) 99 [hep-ph/9912391] [INSPIRE].

[38] M. Carena, S. Heinemeyer, C.E.M. Wagner and G. Weiglein, *Suggestions for benchmark scenarios for MSSM Higgs boson searches at hadron colliders*, *Eur. Phys. J.* **C 26** (2003) 601 [hep-ph/0202167] [INSPIRE].

[39] M. Carena, S. Heinemeyer, O. Stal, C.E.M. Wagner and G. Weiglein, *MSSM Higgs Boson Searches at the LHC: benchmark Scenarios after the Discovery of a Higgs-like Particle*, *Eur. Phys. J.* **C 73** (2013) 2552 [arXiv:1302.7033] [INSPIRE].

[40] J.R. Ellis, J.S. Lee and A. Pilaftsis, *CERN LHC signatures of resonant CP-violation in a minimal supersymmetric Higgs sector*, *Phys. Rev.* **D 70** (2004) 075010 [hep-ph/0404167] [INSPIRE].

[41] S. Berge, W. Bernreuther and S. Kirchner, *Prospects of constraining the Higgs boson's CP nature in the tau decay channel at the LHC*, *Phys. Rev.* **D 92** (2015) 096012 [arXiv:1510.03850] [INSPIRE].

[42] H. Arason, D.J. Castano, B. Keszthelyi, S. Mikaelian, E.J. Piard, P. Ramond et al., *Renormalization group study of the standard model and its extensions. 1. The Standard model*, *Phys. Rev.* **D 46** (1992) 3945 [INSPIRE].

JHEP02(2016)123